UNIVERSITA' DEGLI STUDI DI VERONA

DEPARTMENT OF

Medicine

GRADUATE SCHOOL OF

Life and Health Science

DOCTORAL PROGRAM IN

Inflammation, Immunity and Cancer

WITH THE FINANCIAL CONTRIBUTION OF
Associazione Italiana Ricerca Cancro (AIRC n. 12182)
Italian Ministry of Research (Cancer Genome Project FIRB RBAP10AHJB)

Cycle / year (1° year of attendance) XXIX/2014

TITLE OF THE DOCTORAL THESIS

Landscape of genomic alteration of Pancreatic Neuroendocrine Tumours

S.S.D. MED08
(Please complete this space with the S.S.D. of your thesis – mandatory information)*

Coordinator: Prof./ssa Gabriela Costantin

Signature Gabriela Costantin

Tutor: Prof. Aldo Scarpa

Signature Aldo Scarpa

Doctoral Student: Dott./ssa Ivana Cataldo

Firma Ivana Cataldo

* For the list of SSD please refer to Ministerial Decree of 4th Ottobre 2000, Attachment A *"Elenco dei Settori Scientifico - Disciplinari"* available at: http://www.miur.it/atti/2000/alladm001004_01.htm

UNIVERSITA' DEGLI STUDI DI VERONA

DEPARTMENT OF

Medicine

GRADUATE SCHOOL OF

Life and Health Science

DOCTORAL PROGRAM IN

Inflammation, Immunity and Cancer

WITH THE FINANCIAL CONTRIBUTION OF
Associazione Italiana Ricerca Cancro (AIRC n. 12182)
Italian Ministry of Research (Cancer Genome Project FIRB RBAP10AHJB)
ICGC (International Cancer Genome Project)

Cycle / year (1° year of attendance) XXIX/2014

TITLE OF THE DOCTORAL THESIS

Landscape of genomic alteration of Pancreatic Neuroendocrine Tumours

S.S.D. MED08
(Please complete this space with the S.S.D. of your thesis – mandatory information)*

Coordinator: Prof./ssa Gabriela Costantin

Signature _____

Tutor: Prof. Aldo Scarpa

Signature _____

Doctoral Student: Dott./ssa Ivana Cataldo

Firma _____

* For the list of SSD please refer to Ministerial Decree of 4th Ottobre 2000, Attachment A *"Elenco dei Settori Scientifico – Disciplinari"*available at: http://www.miur.it/atti/2000/alladm001004_01.htm

Landscape of genomic alterations of Pancreatic Neuroendocrine Tumours
Ivana Cataldo
Tesi di Dottorato
Verona, 31 Dicembre 2016
ISBN ???????

“ Quale mondo giaccia al di là di questo mare non so,
ma ogni mare ha un'altra riva, e arriverò”.

C. Pavese

Contents **pg**

1. Background and Rationale

1.1 *History of Neuroendocrine Tumours*

Neuroendocrine cells were discovered in the 19th century, when the first steps for the identification of these cells with peculiar neuronal and secretive characteristics were done. At the beginning of the 19th century, Ivan Pavlov (1849–1936) and, independently, William Bayliss (1860–1924) and Ernest Starling (1866–1927), gave the first empiric demonstrations of the "chemical messenger theory" proving the existence of tissue specific substances (hormones) able to influence specific organs responses. Starling himself recognized that pancreatic gland secretion regulated by both hormones and nerves, thus recognising the existence of a gastroenteropancreatic (GEP) neuroendocrine system. During the following years many scientists dedicate themselves to analyse and characterize the neuroendocrine physiology and pathology and in 1867, Theodor Langhans (1839–1915) first described an intestinal neoplasm with "unusual appearance". It was only 40 years later that a pathologist, Siegfried Oberndorfer (1876–1944), named these "unusual tumours" as "karzinoide" to differentiate them from true carcinoma. Since their identification, several studies have occurred describing the high heterogeneity of these tumours in term of both morphology and biology(1).

1.2 *Epidemiology of Pancreatic Neuroendocrine Neoplasms*

Neuroendocrine tumours are considered rare neoplasm with an overall incidence of 0.2/100.000 person per year(2) although, in the last three decades, it was registered a considerably increase of their incidence (**Fig 1**) probably also related to the improvement of clinical and pathological diagnostic performance(3). The estimated incidence is expected to reach to 8/100,000 today with no significant difference between gender. Median age at diagnosis is usually 50 years, although they can occur at any age(4).

Pancreatic neuroendocrine neoplasms (PanNENs) represent the second most common epithelial cancer of the pancreas with an incidence of 5% among all pancreatic neoplasm(3) and 10-year survival of about 45%(5).

1.3 *Classification, Staging and Histopathological Diagnosis*

PanNENs are to date classified according to WHO 2010 classification(5) (**Fig 2a**) which defines three different groups of grading (G) according alternatively to the proliferative fraction of neoplastic cells, assessed by immunohistochemical evaluation of nuclear stain for ki67, or mitotic count, consisting with: pancreatic neuroendocrine tumour low grade (PanNET-G1), PanNET-G2 (intermediate grade) and pancreatic neuroendocrine carcinoma (PanNEC-G3) (Fig 2a). PanNEC-G3, although rare, are characterized by a poorly differentiated morphology and an invariably lethal outcome with a mortality of about 100%; conversely the vast majority of pancreatic neuroendocrine neoplasms are PanNETs G1 or G2, and despite the well differentiated morphology they all possess a malignant potential and an often unpredictable clinical behaviour, varying from indolent to highly malignant.

Pan-NET G1-G2 are well differentiated neoplasms, characterized by various histological architectural patterns (nesting, pseudoglandular, trabecular, solid, tubule-acinar) and are composed by well-differentiated uniform cells, with a discrete amount of eosinofilic/amphophilic cytoplasm and round to oval nuclei, with a characteristic "salt-and-pepper" chromatin distribution. Occasionally, rabdoid, clear-cell or oncocytic variants have been identified along with a "pleomorphic" one characterized by large and irregular nuclei. The amount of stroma is variable with different grade of fibrosis and necrosis is usually very limited or absent. Pan-NETs usually express cytokeratins (CK8-18, CK19) and neuroendocrine differentiation markers at immunohistochemical analysis (like CD56, Sinaptophysin, CromograninA, Neuronal Specific Enolase). Hormone secretion can be also demonstrated although functional NETs are defined on the basis of clinical symptoms rather than immunohistochemical stains for hormones. Specific architectural and morphological pattern are not usually related to specific hormones secretion, although in case of insulinoma, amyloid deposits can be detected and somatostatin secreting tumours usually show a gland-like structures containing psammoma bodies.

Pan-NEC are high grade neoplasms characterized by a large nest or solid sheet of poorly differentiated cells (small cell or large cell NEC according to size) with scant cytoplasm, irregular nuclei with evident nucleoli. Necrosis can be extensive.

In recent years the hypothesis of a different pathogenesis among PanNETs and PanNECs has been provided by several evidences that demonstrated the existence of different molecular alterations between NET and NEC(6) and in the next years these findings will probably modify the current classifications.

Nevertheless, altogether these tumours are staged according to TNM/AJCC 7th edition, that include information about size and potential infiltration of neighbouring organs and structure (T), nodal status (N) and distant metastasis (M) **(Fig 2b**)(7). An updating of the current classification has been proposed by ENETS (European Neuroendocrine Tumours Society) (Fig 2b)(8). In the last months the AJCC/UICC classification of PanNENs has been updated (8th edition), although it will become effective since 1st January 2018, thus in the present analysis we referred to the 7th edition.

1.4 *Pathogenesis and Molecular Pathology*

PanNETs develop from cells with neuroendocrine characteristics belonging to pancreatic islets of Langerhans, although, like the other NETs, are an heterogeneous group of neoplasms in term of both clinico-pathological characteristics and biological behaviour and their prognostic stratification is often challenging(9).

NETs can occur sporadically or in the setting of clinical syndromes. Characteristically PanNETs can be related to multiple endocrine neoplasm type 1 (MEN1) syndrome in 10-20% of cases, although several syndromes have been described to be associated with the occurrence of PanNETs (namely von Hippel-Lindau disease and less commonly neurofibromatosis type 1, tuberous sclerosis complex and in families with germline mutations in cyclin-dependent kinase inhibitor genes)(10).

Genes involved in the abovementioned syndromes can also act as drivers in sporadic PanNETs tumorigenesis. Lessons from the analysis of these familial syndromes along with reports on genetic and epigenetic alterations of non-familial NETs, have increased our understanding of mutational mechanisms that entail the pathogenesis of neuroendocrine tumours.

MEN1 gene, located on chromosome 11q13 and encoding for menin, was found to be altered by inactivating mutations coupled with loss of heterozigosity of the wild-type allele(11), in about 35% of cases of PanNETs(12). Furthermore in a recent study on 169 PanNETs, Corbo et al, reported an altered menin expression in 80% of cases while known molecular alteration of *MEN1* were identified at low frequency (in 35% of cases) only partly explaining the higher rate of protein dysfunction(13).

Along with *MEN1* mutations, inactivating mutation in *DAXX* (death-domain-associated protein) and *ATRX* (alpha thalassemia/mental retardation syndrome X-linked) have been described in about 43% of PanNETs, as well as activating mutations in the PI3K-AKT-mTOR pathway(12). Less frequent mutations have been detected in *ATM* (5.5%) and *KIT* (2.7%)(14) and *VHL* and *PTEN(*15) while no mutations have been identified in genes commonly mutated in pancreatic ductal adenocarcinoma (i.e. KRAS, TP53, CDKN2A and SMAD4)(16).

DAXX and ATRX belong to the chromatin remodeling pathway and mutually exclusive mutations have been reported in about 40% of sporadic, variably associated with *MEN1* mutations(12, 17). DAXX and ATX mutation are correlated with alternative telomerase independent telomere maintenance mechanism named alternative lengthening of telomeres (ALT)(18). DAXX/ATRX mutation and ALT have been identified in PanNETs and not in neuroendocrine micro adenomas; furthermore these abnormalities have been observed in higher grade (G2 versus G1) and larger sized cases (tumor diameter >3 cm)(19) along with reduced survival(20), suggesting the late occurrence of these alterations in PanNETs tumorigenesis.

MTOR-pathway deregulation is also considered another important pathogenic mechanism in PanNETs, determining an important stimuli to cell

survival, cell proliferation, metabolism and angiogenesis; this pathway encompass several genes that have been described to be potentially altered in PanNETs (like *PTEN*, *AKT*, *PI3KCA*, *MEN1*, *VHL*, *NF1*, *TSC1* and *TSC2*, several tyrosine kinases receptors)(10). Furthermore numerous reports have highlighted the role of m-TOR pathway activation as poor prognostic indicator in PanNETs(21-23). Although the mTOR inhibitor Everolimus is FDA approved for the treatment of advanced PanNET(24), selection of patients who will benefit of this therapy based on molecular analysis is yet to be developed.

Copy number analysis identified several chromosomal aberrations common in PanNETs, mainly loss of chromosome 11q(containing the genes MEN1, BRCA2 and ATM), 11p and 6q, as well as gains in 17q (NEU/ERB2), 7q and 20q (AURKA, cMET) along with LOH at specific chromosomal loci (PTEN, MEN1 and PHLDA3)(10).

1.5 *Rationale*

Despite the great advantages in the knowledge of molecular alterations that unveil pathogenic mechanism along with some prognostic and predictive factors, our current understanding of the molecular pathology of PanNETs, is insufficient for an appropriate clinical management, where the most important clinical challenge is to predict the aggressiveness of individual tumours in order to select patients for the more appropriate therapy differentiating who will benefit from early aggressive therapy from those patients with indolent disease that conversely would be exposed to inadvertent overtreatment.

Here, a comprehensive molecular analysis of 102 clinically sporadic PanNETs belonging from a multi-centric cooperative group (ARC-Net Research Centre at Verona University, Australian Pancreatic Cancer Genome Initiative -APGI, and Baylor College of Medicine as part of the ICGC, www.icgc.org) defines their molecular pathology and identifies several candidate novel mechanisms that activate mTOR signalling including novel gene fusion events. We uncover an important role for germline *MUTYH* variants through a novel G:C>T:A mutational signature. Moreover, we

identify a larger than anticipated germline contribution to clinically sporadic PanNET, delineating future challenges in the clinical assessment of susceptibility.

2 Results and Discussion

2.1 *Cohort Characteristics*

Patients were recruited and consent for genomic sequencing obtained as part of the International Cancer Genome Consortium (www.icgc.org). All cases were classified according to WHO criteria updated to ENETs classifications(5, 8).

The discovery cohort included 98 resected PanNETs (**Table 1**) with an average tumour content of 82%(25); 36 cases were classified as G1, 57 as G2, and 5 as G3. Additional 62 cases of PanNETs and one colon cancer from a MUTYH associated Polyposis (MAP) were included in the study as validation cohort, of which 4 PanNETs and the CRC underwent whole genome sequencing to validate mutational signatures (data not shown), while all the 62 PanNETs were also analysed by targeted next-generation sequencing and FISH to validate somatic/germline variants and fusion transcript respectively.

2.3 *Study design*

The analyses were conducted on a discovery cohort of 98 PanNETs and on a validation set of an additional 62 PanNETs and 1 colorectal cancer.

The discovery cohort underwent whole genome sequencing (WGS) for the examination of telomere length, structural variants, somatic/germline variants and mutational signature analysis. C-tailing qPCR was performed on 86 cases of the discovery set in order to validate WGS-telomere length analysis and to detect the presence of alternative telomere lengthening (ALT) mechanism. SNP array analysis was performed on the whole discovery cohort in order to detect copy number variation.

The presence of specific chromosomal structural variants detected by WGS were validated by RNAseq. Fluorescent in situ hybridization (FISH) using a break-apart probe, was used to demonstrate the presence of *EWSR1* rearrangements in 4 cases (3 from discovery and 1 from validation PanNETs cohort). Finally to validate the presence of fusion transcript related to *EWSR1*

rearrangement, RT-PCR analysis was performed, followed by Sanger sequencing of the detected products.

Amplicon sequencing was performed on the 62 cases of validation set to confirm the WGS data on somatic variants and *MUTYH* mutational signature. Four PanNETs of validation cohort and the colorectal cancer case underwent WGS to validate mutational signature data and germline/somatic variants detected by WGS.

2.3 *Mutational mechanisms*

PanNETs are characterized by a lower mutation burden (0.82 per megabase, range 0.04-4.56) compared with their exocrine counterpart(26) (pancreatic ductal adenocarcinoma: mean 2.64, range 0.65–28.2), with the 98 PanNETs containing 258,678 high confidence somatic point mutations and indels.

Non-negative Matrix Factorization(27) defined 5 robust mutational signatures (**Fig. 3a**) consisting with: the unknown aetiology 'Sanger signature 5'(27) reported in many tumour types, Deamination signature, AID/APOBEC signature, BRCA signature and a previously "undescribed" signature, named "novel signature". The germline heterozygous *APOBEC3A-3B* deletion identified in 13 cases resulted prevalent only in 2 PanNETs indicating that this signature, implicated in APOBEC-induced mutation(s) in breast cancers(28), plays a minor role in PanNETs (Fig. 3a). Only one case harbouring a pathogenic germline *BRCA2* mutation (Fig. 3c) carried a highly prominent BRCA-deficiency signature (>2mutations/Mb), with high genomic instability similarly to what previously described in BRCA-deficient breast(29), pancreatic ductal(26), ovarian(30) and oesophageal carcinomas(31). The novel mutational signature, composed of G:C>T:A transversions, resulted predominant in 5 PanNETs (range 0.2-4.2 mutations/Mb) (Fig. 3a)**,** bearing a known pathogenic or novel-damaging germline mutation in the Base-Excision-Repair gene *MUTYH*, coupled with LOH (Fig. 3d). This pattern of biallelic *MUTYH* inactivation was not observed in 100 pancreatic ductal adenocarcinomas using the same analysis

pipeline(26). Germline biallelic inactivation of *MUTYH* is involved in the pathogenesis of colorectal *MUTYH* associated polyposis (MAP), an autosomal recessive syndrome associated with somatic G:C>T:A transversions in the *APC* gene, the driver of colorectal polyps(32). To verify our findings, amplicon sequencing of *MUTYH* on 62 additional PanNETs identified 3 tumours bearing pathogenic germline mutations coupled with LOH. Whole genome analysis revealed that these three tumours displayed the same novel mutational signature (Fig. 3b). Interestingly, the two missense *MUTYH* mutations identified in the Italian cohort (c.527A>G, p.Y176C; c.1178G>A, p.G393D) are the most common MAP-linked variants in populations of European origin and have been shown to be founder mutations in a recent haplotype analysis of 80 MAP families from Italy and Germany(33). Finally, WGS of a colonic tumour from a MUTYH associated polyposis patient confirmed that this signature indicates *MUTYH* deficiency (Fig. 3b). These data suggest that, in addition to predisposing to colonic, gastric and a variety of non-gastrointestinal cancers(34), *MUTYH* deficiency plays a role in PanNETs.

Chromothripsis defined by the accumulation of thousands of clustered chromosomal rearrangements in a single event and in localised and confined genomic regions or in one or a few chromosomes (35), was detected in 9 tumours (9%), consisting with the presence of clusters of breakpoints (**Fig. 4**). All those cases displayed structural variations and copy-number changes (data not shown) and interestingly, 4 out of 9 tumours had recurrent catastrophic rearrangements on chromosome 11q (Fig. 4b), all involving 11q13, and 2 led to loss of *MEN1*. Notably, despite *TP53* being considered a hallmark of chromothripsis(36), no *TP53* mutations were present in tumours with genomic catastrophes in PanNETs.

2.4 *Germline Mutations*

The discovery of germline deleterious mutations of *MUTYH* and *BRCA2* prompted us to screen the germline of all patients for mutations in DNA

damage repair genes or genes associated with hereditary syndromes (data not shown).

In the case of known neuroendocrine predisposition genes, 6 patients carried either known pathogenic or novel deleterious germline *MEN1* mutations (4 frameshifts, 1 splice site-mutation, and 1 copy-number loss).

A single novel truncating *CDKN1B* germline mutation was identified (Q163X). *CDKN1B* germline mutations cause Multiple Endocrine Neoplasia Type 4(37) and its somatic mutations have been recently described in small-intestinal NET(38). In addition a single, novel, pathogenic germline mutation was identified within *VHL*, a negative regulator of hypoxia signalling known to promote neuroendocrine proliferation and PanNETs development(39). Germline alterations were coupled with somatic LOH in all cases.

CHEK2, belonging to DNA-damage repair pathway and a known tumour suppressor in breast and other cancer types, had predicted damaging germline variants in 4 cases (4%): a nonsense mutation (c.58C>T, Q20X), a 15bp in frame deletion (c.246-260del, p.D77-E82del), a missense mutation in exon 2 implicated in prostate cancer predisposition (rs121908702, c.844G>A, p.E282K)(40) and a missense variant in exon 4 (c.529G>C, p.D177H). Mutation modelling predicted these variants to be damaging.

2.5 *Somatic driver mutations*

A total of 15,751 somatic coding mutations of which 7,703 non-silent, were detected in 2,787 genes (data not shown). Sixteen significant, recurrently-mutated genes were defined using IntOGen(41) analysis (Q-value <0.1) (**Fig. 5a**).

As previously reported, *MEN1* was the most frequent mutated genes in 37% of tumours (**Fig. 5b**). Mutually exclusive inactivating mutations of *DAXX* and *ATRX* were found in 22 and 11 samples, including a structural rearrangement of *ATRX*, respectively.

Members of the mTOR pathway *PTEN* (n=7) and *DEPDC5* (n=2) were also significantly mutated. *PTEN* mutations were mutually exclusive to *TSC1* (n=2) and *TSC2* (n=2), other negative regulators of mTOR signalling (Fig.

5a). Mutations of the tumour suppressor gene *DEPDC5* have not been previously described in PanNETs; hence we surveyed additional 62 PanNETs cases (data not shown) and identified additional 2 tumours harbouring *DEPDC5* mutations, which resulted to be again mutually exclusive to *PTEN* (n=3) and *TSC2* (n=3) also in this validation set (data not shown).

Consistent with literature data, deleterious *TP53* mutations were uncommon (n=3). Among the genes not meeting the significance threshold by IntOGen, *SETD2*, an histone modifier, resulted mutated in 5 samples (Fig. 5a). Multiple independent *SETD2* mutations were observed in presumed sub-clones of one tumour (a nonsense at 3%, a missense at 14% and a frameshift at 11% allelic frequency), suggesting strong selection for *SETD2* inactivation in that particular tumour, similarly to previous observations in renal cell carcinoma(42).

2.6 *Copy number changes*

Copy number analysis revealed the presence of 4 discrete groups based on arm length copy number patterns (**Fig. 6**). These were classified into: 1) recurrent pattern of whole chromosomal loss (RPCL); 2) limited copy number events, many of which were losses affecting chromosome 11; 3) polyploid; and 4) aneuploid (Fig. 6a and b). Interestingly, the RPCL subtype consistently presented loss of specific chromosomes (Fig. 6) and was significantly enriched in G2 PanNETs (P=0.0247, Chi-square test). The polyploid group had the highest somatic mutation rate ($P \leq 0.002$, Mann-Whitney test) with an average of 1.98 mutations/Mb (**Fig. 6c**).

Recurrent regions of gain and loss (**Fig. 6d**) included broad regions of loss containing known neuroendocrine tumour suppressors *MEN1* (chromosome 11q13.1) and *CDKN2A* (chromosome 9q21.3), while focal losses highlighted potential tumour suppressor roles for *EYA1* (chromosome 8q13.3) a known target of *MEN1(43)*, *SFMBT1* (chromosome 3p21.1) a key component of histone modification machinery implicated in cancer(44), and *RABGAP1L* (chromosome 1q25.1), a gene frequently deleted in neurofibromas(45). Significant, recurrently-amplified regions included: *PSPN* (chromosome

19p13.3), a member of the glial cell line-derived neurotrophic factor family, known to activate PIK3CA-signalling via RET and upregulated in thyroid medullary cancers(46, 47); and *ULK1* (chromosome 12q24.33), a serine-threonine kinase that is involved in mTOR regulated autophagy(48).

2.7 *Chromosomal rearrangements*

Structural rearrangements are less common in PanNETs (mean, 29 events per tumour; range 3–216) (data not shown) compared to pancreatic ductal adenocarcinoma (119 per tumour; range 15–558)(26). Inactivation of tumour suppressor genes through rearrangement occurred in *MTAP* (n=4), *ARID2* (n=5), *SMARCA4* (n=3), *MLL3* (n=3), *CDKN2A* (n=1), and *SETD2* (n=1).

Rearrangements can also generate oncogenic drivers through in-frame gene fusions. 66 somatic fusions capable of expressing in-frame chimeric genes were identified (data not shown). Interestingly, *EWSR1* gene was involved in fusion events in 3 PanNETs. Two tumours possessed in-frame *EWSR1-BEND2* fusion genes, which were expressed as mRNA (**Fig. 7a and b**), defining *BEND2* as a novel *EWSR1* fusion partner. Noteworthy, *BEND2* was recently reported as a fusion partner of *MN1*, encoding for a transcriptional activator involved in meningioma development, in CNS high-grade neuroepithelial tumour(49). One tumour contained an *EWSR1* exon 7 - *FLI1* exon 6 gene fusion confirmed by RNAseq (**Fig. 7c**). *EWSR1-FLI1* fusions occur characteristically in Ewing's sarcomas(50, 51) although has been recently reported in other cancers(52) and rarely in pancreas or gastrointestinal tract(53). The 3 fusion events involved the region of *EWSR1* that is most susceptible to breakage/translocation in a variety of soft tissue tumours and Ewing sarcoma, and can be detected by fluorescent in situ hybridization (FISH) analysis using break-apart probes for *EWSR1* (Fig. 7a-c). By applying FISH on the 62 cases of the validation cohort, we identified an additional PanNET with positive split signals due to an *EWSR1* exon 7 - *FLI1* exons 5 fusion (Type II) confirmed at the mRNA level (Fig. 7d). Ewing sarcoma is a distinctive poorly differentiated high grade round cell sarcoma that most often (but not exclusively) affect children and young adults (< 25

years); they characteristically develop in soft tissue and bone and are exceedingly rare in other sites. Ewing tumours, typically show a strong membranous expression of membrane glycoprotein CD99(54) and specific inactivation of tumour suppressor genes (STAG2, TP53 and CDKN2A) or chromosomal copy-number variations (gains of chromosome 8 and 1q)(55-57). Conversely the 4 PanNETs cases bearing *EWSR1* fusions had morphological and immunophenotypical features typical of PanNET (i.e. strong immunoreactivity for chromogranin and synaptophysin), with absent to faint staining for CD99, lack Ewing's sarcoma typical molecular alterations while showed characteristic PanNETs mutations (in *MEN1*, *ATRX* and TSC2). Nonetheless, the 3 cases of the discovery cohort resulted metastatic at diagnosis with a relatively short survival for PanNETs (25 months for #0993, 51.5 months for #0152, and 7 months for #0457), suggesting that those fusions possibly identify more aggressive subtypes of PanNETs. Furthermore the result of CD99 immunohistochemical analysis on a subset of discovery cohort cases (54 PanNETs) and on the validation cohort, showed that 35 (30%) cases immunostained for CD99, 18 (15%) of which had a very strong signal; however, none of these cases had FISH split signals related to EWSR1 rearrangement. CD99 is generally used to guide diagnosis of Ewing sarcoma. Our data, along with further literature reports, highlight expression of this antigen in a significant fraction of neuroendocrine tumours of different anatomical sites(58, 59) with important implication for histopathological differential diagnosis.

2.8 *Telomere integrity and PanNET molecular subtypes*

Telomere repeat content was quantified using WGS data, and ALT assessed by C-Tailing qPCR in 86 cases. 22 out of 26 *ATRX/DAXX* mutant tumours displayed ALT, and more frequent in *DAXX* (19/22) than *ATRX* (3/22) mutants, in contrast to *in vitro* studies where *ATRX* alterations are more prevalent(60). Biallelic inactivation of *ATRX/DAXX* through LOH was strongly associated with an increase in telomere length ($P<0.0001$, Mann-Whitney test) (data not shown). *MEN1* somatic mutations were also

associated with increased telomere length (P<0.0001, Mann-Whitney test) (data not shown), suggesting a role for *MEN1* in chromosome maintenance.

To better understand the consequences of ALT, somatic telomere content was compared to copy-number and structural variation patterns (**Fig. 8**). The presence of short telomeres was associated with genomic catastrophes and *EWSR1* fusions, consistent with observations that telomere exhaustion plays a role in chromothripsis and bridge-fusion-break events in solid cancers. Interestingly, tumours with ALT were strongly associated with the PanNET-RPCL phenotype, with 16/21 tumours with RPCL displaying ALT. Tumours with ALT, have been previously reported to undergo copy gain and loss in recurrent regions of genes in a panel of human cancer cell lines *in vitro*(60), differently from PanNETs where whole loss of specific chromosomes predominates.

2.9 *Integrated analysis of PanNET cancer pathways*

Four pathways were commonly altered by mutations in PanNETs whose perturbations may define potentially clinically relevant subtypes for a more accurate stratification of therapeutic approaches (Fig. 4):

i) *DNA damage repair*: Germline damaging variants of the base-excision-repair *MUTYH* gene, and homologous recombination genes *CHEK2* and *BRCA2* were present in 11% of patients.

ii) *Chromatin remodelling: MEN1*, *SETD2*, *ARID1A* and *MLL3* were recurrently inactivated, and likely drive widespread transcriptional dysregulation.

iii)*Telomere Maintenance*: Upregulation of TERT and telomere lengthening is a well-established pro-survival mechanism in solid tumours. MEN1 binds the *TERT* promoter and influences the machinery controlling telomere integrity(61). Consistent with previous reports, inactivating mutations in *DAXX* or *ATRX* were present in one third of PanNETs and correlated strongly with somatic telomere repeat content and telomere length (Extended Data 8b and c). Tumours harbouring *DAXX*/*ATRX* mutations were associated with a poor prognosis in the G2 subgroup, and correlated significantly with

mutations in mTOR regulators (**Fig. 9a and b**, **Table 2**). Tumours with unaltered telomere length had a better outcome (Extended Data 10c).

iv) *mTOR signalling activation*: The role of mTOR in PanNETs is well established(12, 23). Inactivating mutations in negative regulators of mTOR signalling (*PTEN*, *TSC2*, and herein reported *TSC1* and *DEPDC5)* were present in 12% of patients, and were associated with a poor prognosis in the G2 subgroup of patients (HR=6.85, 95%CI=1.14 – 41.7; *P*= 0.0353, **Fig. 9d**, Table 1). These may represent putative biomarkers for patient selection for mTOR inhibitor therapy(24). We uncovered 3 potential novel mTOR pathway activation mechanisms: a) inactivating mutations of tumour suppressor *DEPDC5*, encoding a subunit of the GATOR1 complex, a suppressor of mTOR signalling(62), b) a putative mTOR activation mechanism involving *EWSR1* fusion genes, and c) amplification of the *RET* receptor ligand *PSPN*.

Moreover, inactivation of MEN1, that has a broad range of functions, directly impacts on all these 4 key processes(61, 63-65) (**Fig. 10**). *MEN1* encodes the histone modifier Menin and its inactivation drives a variety of phenotypes including widespread transcriptional dysregulation via histone modification(65), activation of mTOR through AKT expression(64), suppression of homologous recombination DNA damage response genes(63) and dysregulation of TERT(61).

3. Conclusion

With the present analysis we describe the mutational landscape of PanNETs and mutational signatures underlying their pathogenesis, including a novel mutational mechanism due to *MUTYH* inactivation. We uncover novel mTOR pathway activation mechanisms including *DEPDC5* inactivation and *EWSR1* fusion events In addition, we identify PanNET subtypes based on global copy number profiles and gene mutations that have potential clinical utility. There are 3 major clinical considerations that have to be done: i) *DAXX/ATRX* and mTOR pathway genes mutational status may serve as novel biomarker for prognostic stratification of intermediate grade PanNETs (G2), the subgroup that represent the most challenging one with the least predictable clinical behaviour. This calls for exploration of its clinical utility in prospective clinical trials. ii) The identification of novel mechanisms that activate mTOR signalling may represent selection biomarkers of therapeutic responsiveness to mTOR inhibitors such as Everolimus, which are currently poorly defined. iii) The discovery of a larger than aspected germline mutation contribution to PanNET development, particularly in patients without a family history, has implications for clinical management for individuals that carry these mutations and have an increased, yet unquantifiable risk of disease.

4. Figures and Tables

Fig.1

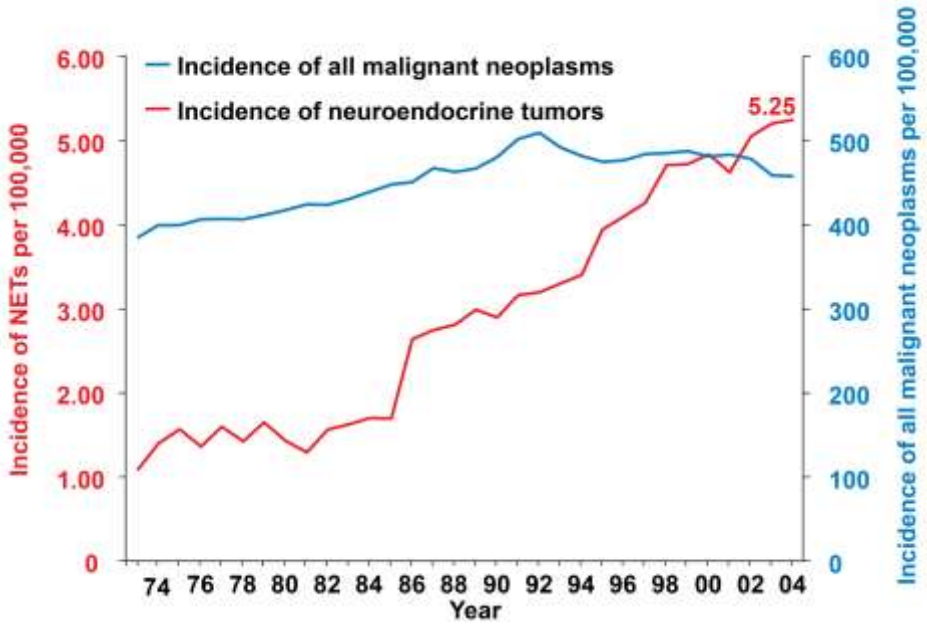

Fig.1 | Incidence of NETs in the past 3 decades. An exceptional increase in NETs incidence have been recorded in the last 30 years. The improvement of clinico-pathological diagnostic tools can partly explain this drastic increment of NETs cases (*from SEER Survival Monograph*).

Fig. 2

a

Grade	Mitotic count, 10HPF[1]	Ki67 index, %[2]
G1	<2	≤2
G2	2-20	3-20
G3	>20	>20

[1]HPF= high power field= 2mm² ,at least 40 fields evaluated in areas of highest mitotic density
[2]MIB1 antibody; % of 2000 cells in areas of highest nuclear labelling

Modified from Kloppel et al, Neuroendocrinology 2009;90:162–166

b

AJCC Staging System 7th ed.		ENETs Staging Classification	
T1	Tumour limited to pancreas, ≤ 2cm	T1	Tumour limited to pancreas, ≤ 2cm
T2	Tumour limited to pancreas, >2cm	T2	Tumour limited to pancreas, 2-4cm
T3	Tumour extends beyond pancreas, without involvement of celiac axis or SMA	T3	Tumour limited to pancreas >4cm or invading duodenum or CBD
T4	Tumour involves celiac axis or SMA	T4	Tumour involves adjacent structures
N0	No regional lymph-nodes metastasis	N0	No regional lymph-nodes metastasis
N1	Regional lymph-nodes metastasis	N1	Regional lymph-nodes metastasis
M0	No distant metastasis	M0	No distant metastasis
M1	Distant metastasis	M1	Distant metastasis

Stage	T	N	M	Stage	T	N	M
IA	T1	N0	M0	I	T1	N0	M0
IB	T2	N0	M0	IIA	T2	N0	M0
IIA	T3	N0	M0	IIB	T3	N0	M0
IIB	T1-3	N1	M0	IIIA	T4	N0	M0
III	T4	N0-1	M0	IIIB	Any T	N1	M0
IV	Any T	Any N	M1	IV	Any T	Any N	M1

SMA: superior mesenteric artery; CBD: common bile duct

Fig. 2 | Grading and Staging of PanNETs. a. Grading of PanNETs according to WHO 2016. **b.** Comparison between AJCC/TNM staging system and ENETs-modified proposal for TNM.

Fig. 3

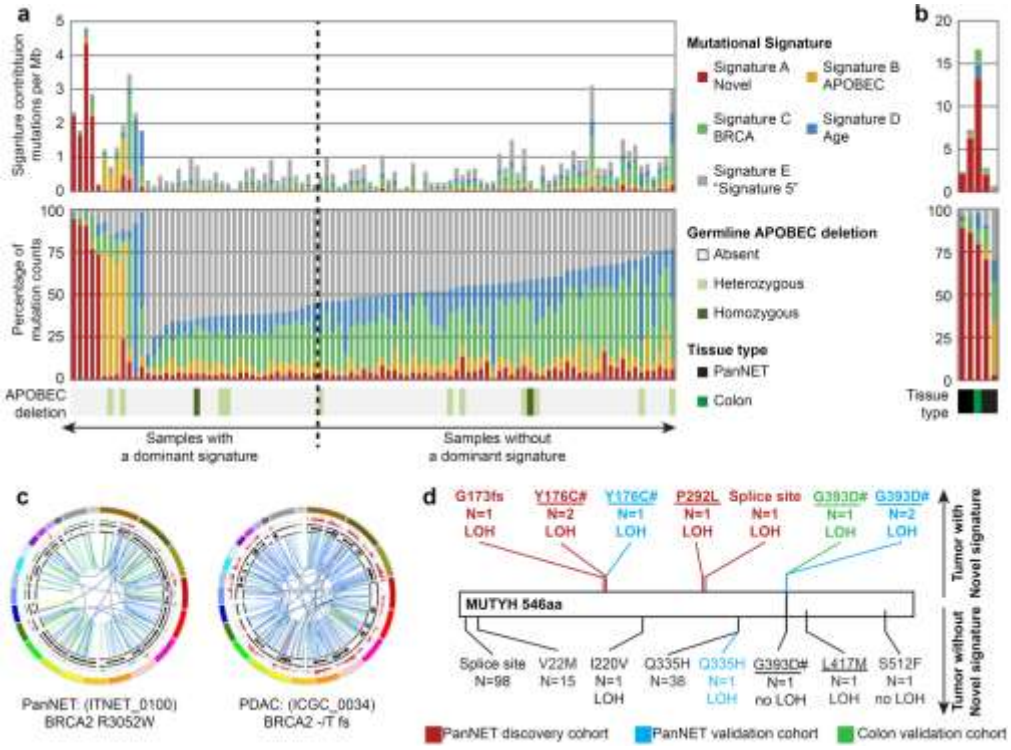

Fig. 3 | Mutational signatures in pancreatic neuroendocrine tumours. a Five signatures (A-E) were identified in 98 PanNET samples**.** Signature A is novel and has been named MUTYH because all tumours dominated by this signature carried a germline inactivating mutation in *MUTYH* with concurrent loss of the wild-type allele; signatures B to E have been previously described and are reported with their given names. Tumours with a high MUTYH, APOBEC, BRCA or Age signature showed a higher number of mutations per Mb. **b** Validation of MUTYH signature in 4 additional PanNETs and 1 colon tumour. Three PanNET and the colon tumour contained a dominant MUTYH signature and harboured a germline damaging *MUTYH* mutation with concurrent loss of the wild-type allele, while a PanNET with a benign *MUTYH* variant did not contain the signature. **c** The tumour with the BRCA signature contained a *BRCA2* germline variant (R3052W) and genomic instability as seen in pancreatic ductal adenocarcinoma. **d** Variants displayed above the MUTYH protein were associated with the MUTYH signature and contained somatic biallelic inactivation of the *MUTYH* gene (highlighted in

bold), those below were not and are either benign or showed no loss of the wild-type allele. Variants reported by Clinvar as pathogenic (#) are shown. Variants predicted by SIFT as deleterious and Polyphen as probably damaging are underlined. All mutations shown are for the transcript ENST00000372098.3 and protein ENSP00000361170.3.

Fig. 4

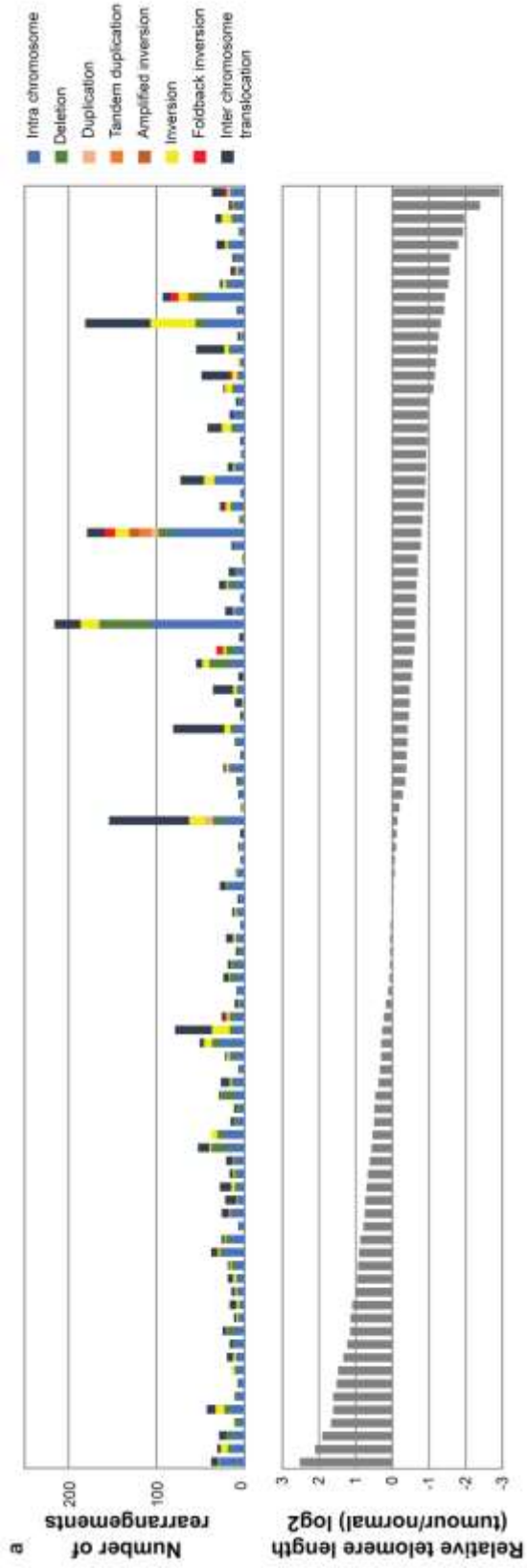
a
Number of rearrangements
200
100
0
Intra chromosome
Deletion
Duplication
Tandem duplication
Amplified inversion
Inversion
Foldback inversion
Inter chromosome translocation
Relative telomere length (tumour/normal) log2
3
2
1
0
-1
-2
-3

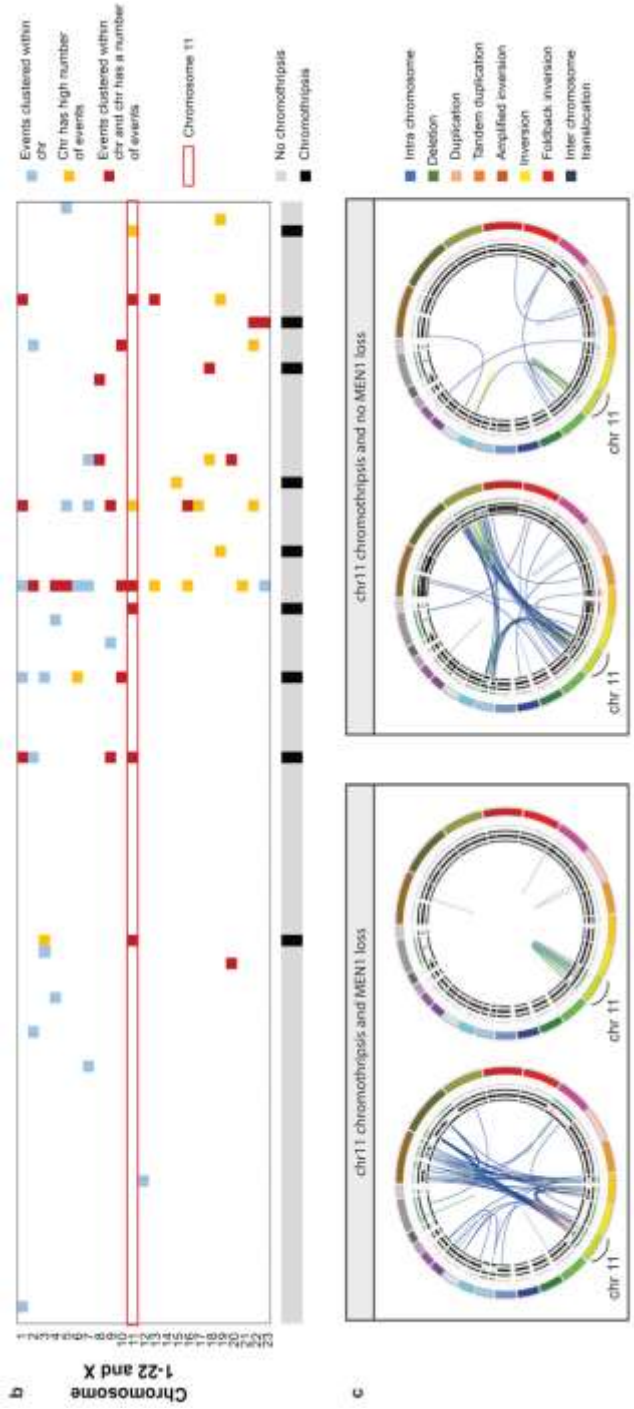

Fig. 4 | Structural rearrangements in pancreatic neuroendocrine tumours. a Upper panel: the number and type of somatic structural rearrangements in each tumour. Lower panel: tumours with more events tended to have longer telomeres. **b** Two methods were used to determine clusters of somatic structural rearrangement breakpoints. Orange squares:

chromosomes with a significant cluster of events as determined by a goodness of fit test against the expected distribution ($p<0.0001$, Kolmogorov–Smirnov test). Blue squares: chromosomes deemed to harbour a high number of breakpoints because they had a chromosomal breakpoint per Mb rate which exceeded the 75th percentile of the chromosomal breakpoint/Mb rate for the cohort by 5 times the interquartile range. Red squares: chromosomes where both these criteria were met. Clusters of events were reviewed and 9 tumours were found to harbour regions of chromothripsis. **c** Recurrent chromothripsis for chromosome 11 was detected in 4 tumours. The chromothripsis event caused loss of the *MEN1* gene locus in 2 of these samples.

Fig. 5

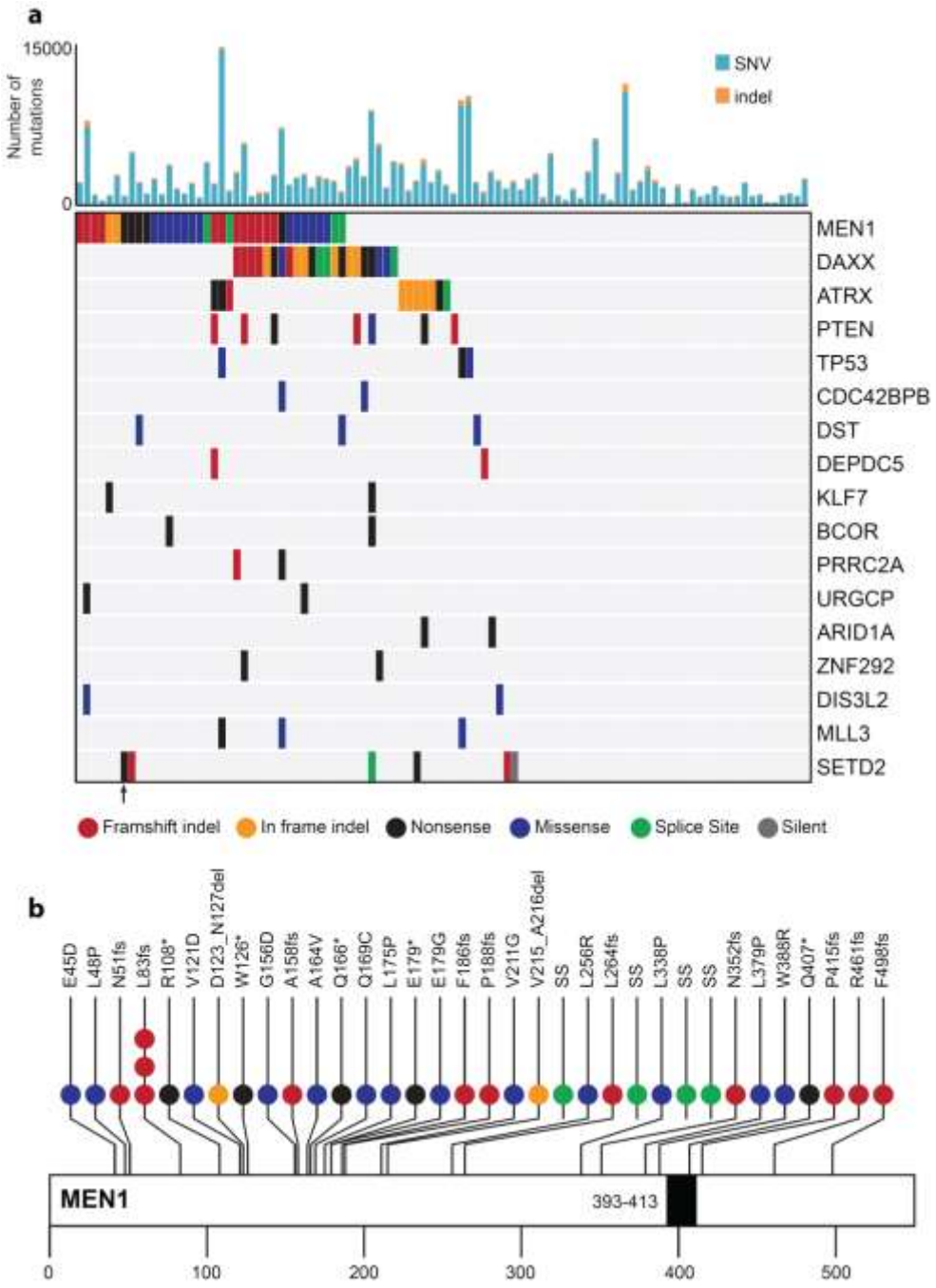

Fig. 5 | Recurrently mutated genes in pancreatic neuroendocrine tumours. **a** The number of SNVs and indels within the genome of each patient (n=98) is shown in the histogram. The driver plot displays the somatic mutations in key genes or those identified as significantly mutated (Intogen

Q-value <0.1). *SETD2* is also reported, although its Q-value was 0.15, as it was recurrently inactivated in 6 samples and multiple independent deleterious *SETD2* mutations were observed in one tumour (a nonsense present at 3%, a missense at 14%, and a frameshift at 11 %, only the nonsense is shown but the case is highlighted with a black arrow), suggesting strong selection for *SETD2* inactivation in that tumour. **b** Somatic mutations in MEN1 are predominantly nonsense mutations or insertions-deletions causing frame shift and premature protein termination, and occur throughout the protein.

Fig. 6

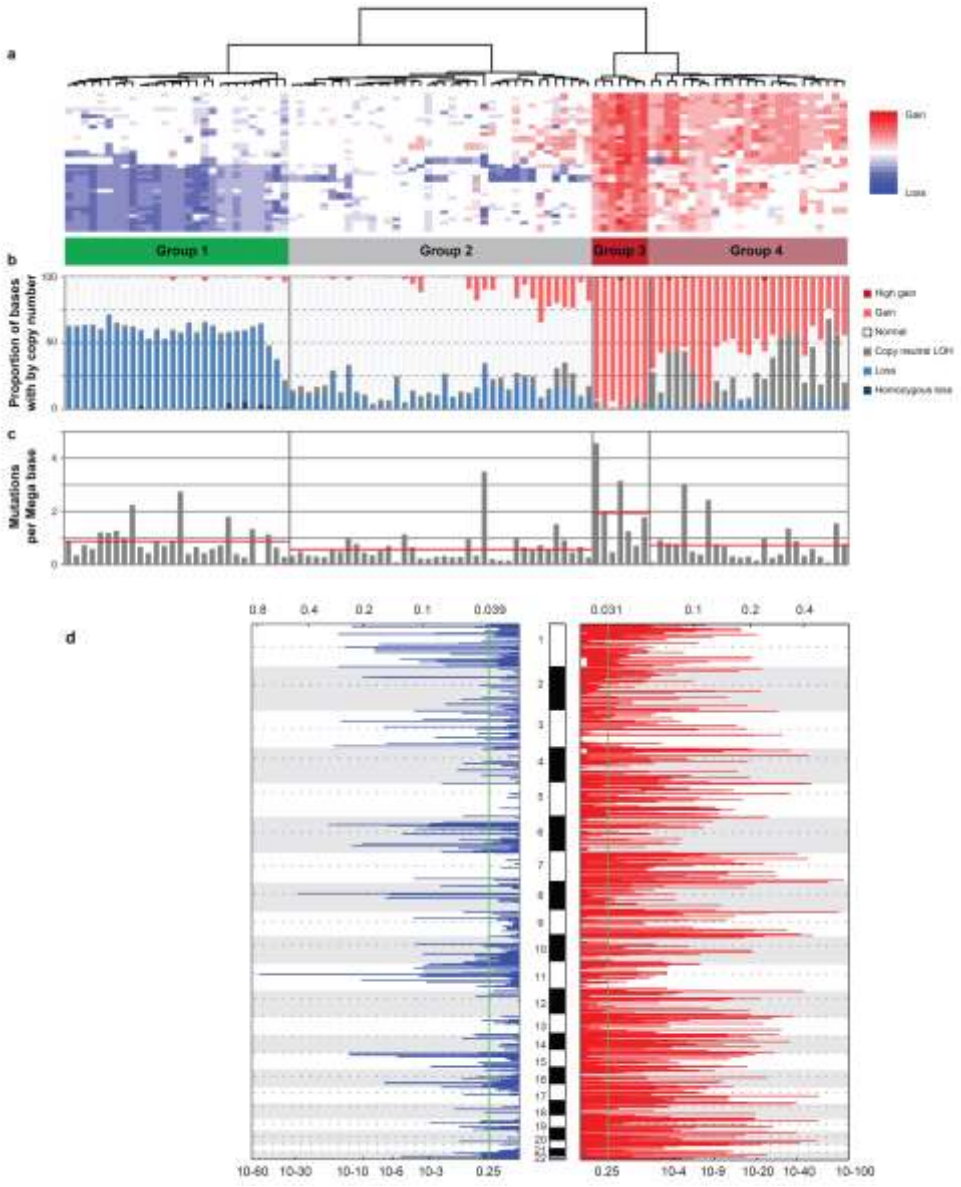

Fig. 6 | Genome characteristics of pancreatic neuroendocrine tumours. Copy number was determined using Illumina SNP arrays in a cohort of 98 PanNETs. **a** Copy number events were mainly comprised of whole chromosome arm loss or gain. Cluster analysis of the chromosome arm level copy number state stratified the tumours into 4 subtypes: Group 1: recurrent pattern of whole chromosomal loss, affecting specific chromosomes (1, 2, 3, 6, 8, 10, 11, 15, 16 and 22); Group 2: samples with limited number of events, many of which with loss affecting chromosome 11; Group 3: polyploid tumours, with gain of all chromosomes; and Group 4: aneuploid tumours,

containing predominantly whole chromosome gains affecting multiple chromosomes). **b** The proportion of bases within the genome affected by copy number change. **c** The mutations per Megabase (SNPs and small insertion deletions) and **d** GISTIC analysis showing recurrent gains (red) and losses (blue) of the entire cohort.

Fig. 7

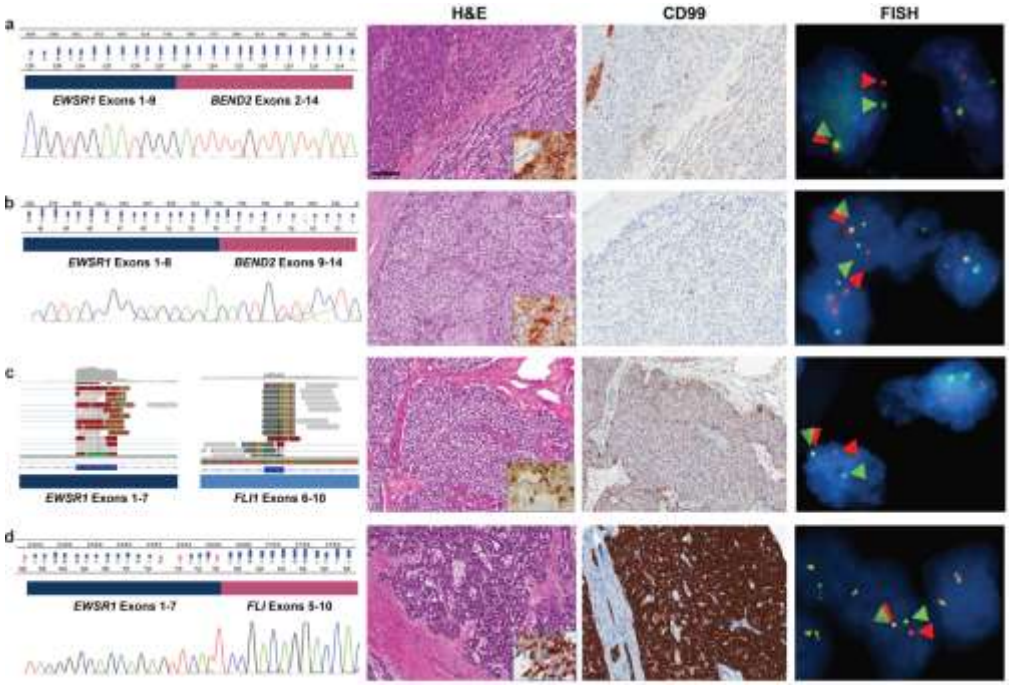

Fig. 7 | *EWSR1* gene fusions in pancreatic neuroendocrine tumours. a and **b** Somatic fusion events between *EWSR1* and *BEND2* confirmed in RNA by capillary electrophoresis of RT-PCR products. Representative sections showing typical PanNET morphology (H&E) and immunoreactivity for the neuroendocrine marker Chromogranin A (inset), lack of immunostaining for CD99, and positive *EWSR1* split signals (arrowheads) detected with fluorescent in situ hybridization (FISH). **c** Somatic fusion event between *EWSR1* and *FLI1* confirmed by RNAseq. Representative sections showing typical PanNET morphology (H&E) and immunoreactivity for Chromogranin A (inset), faint immunoreactivity for CD99, and positive *EWSR1* split signals (arrowheads) at FISH. **d** Somatic fusion event between *EWSR1* and *FLI1* confirmed by capillary electrophoresis of RT-PCR products. Representative sections showing typical PanNET morphology (H&E) and immunoreactivity for Chromogranin A (inset), strong immunoreactivity for CD99, and positive *EWSR1* split signals (arrowheads). Scale bar represents 100µm. Insets, 600x magnification.

Fig. 8

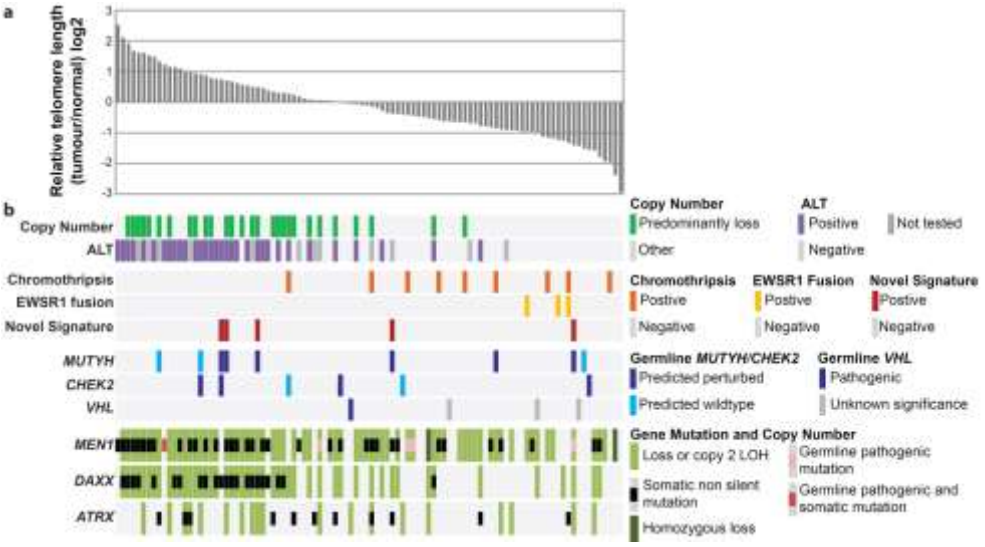

Fig. 8 | Mutational processes in pancreatic neuroendocrine tumours. a Telomere length was estimated using whole genome sequencing in a cohort of 98 PanNETs. The relative telomere length in each tumour compared to the matched normal is shown as log2. A total of 24 tumours contained telomeres which were 1.5x longer than matched normal DNA and 36 contained telomeres which were 1.5x shorter compared to matched normal DNA. **b** Most of the tumours with long telomeres had ALT and 13 of the tumours contained genomes with large amounts of whole chromosome arm losses. Somatic mutations in *DAXX/ATRX* were strongly associated with an increase telomere length ($p<0.0001$, Mann-Whitney test). Tumours with short telomeres contained fewer mutations in *DAXX/ATRX* and more chromothripsis events or *EWSR1* gene fusions.

Fig. 9

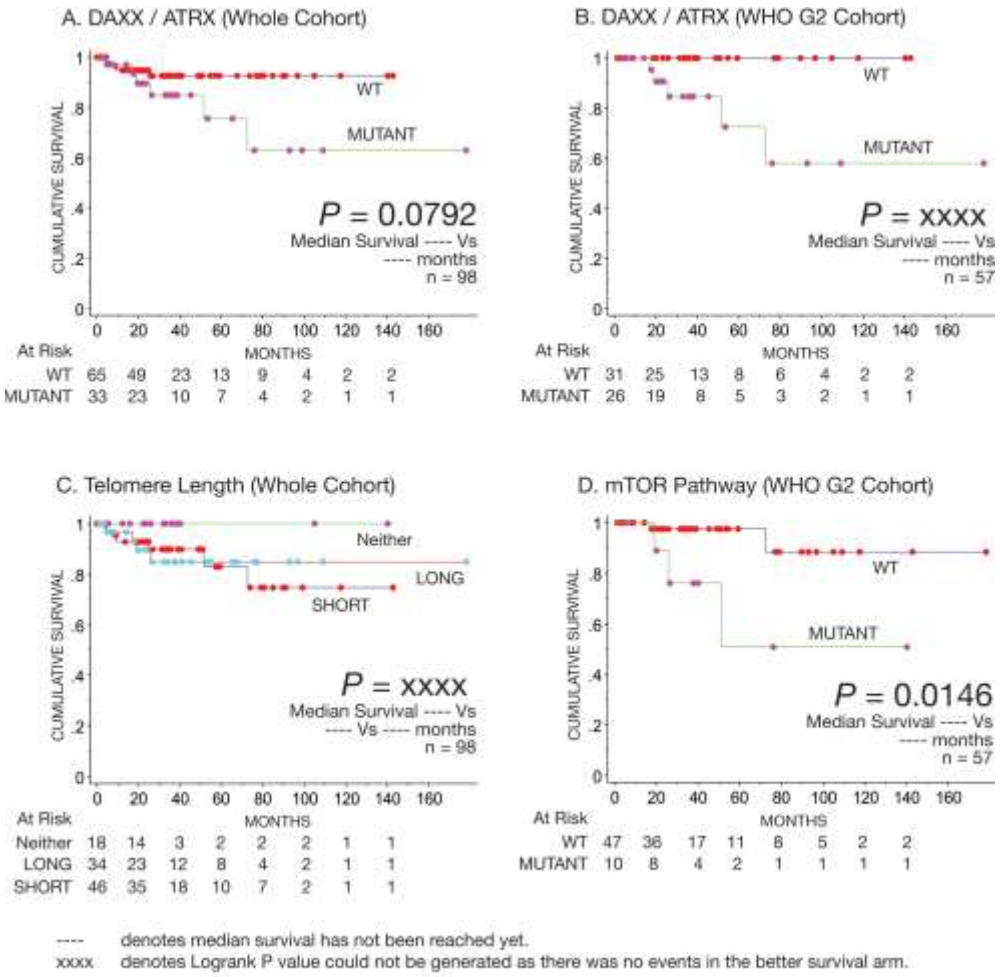

Fig. 9 | Genomic events associated with outcome. Kaplan-Meier survival curves demonstrating: **a** tumours harbouring *DAXX/ATRX* mutations had a poor prognosis in the whole cohort and **b** in the G2 cohort. **c** tumours with telomere length that are neither short or long had a better prognosis, and **d** tumours harbouring mutations in genes that activate mTOR pathway had a poor prognosis in the G2 cohort (Chi-squared test was used in all instances).

Fig. 10

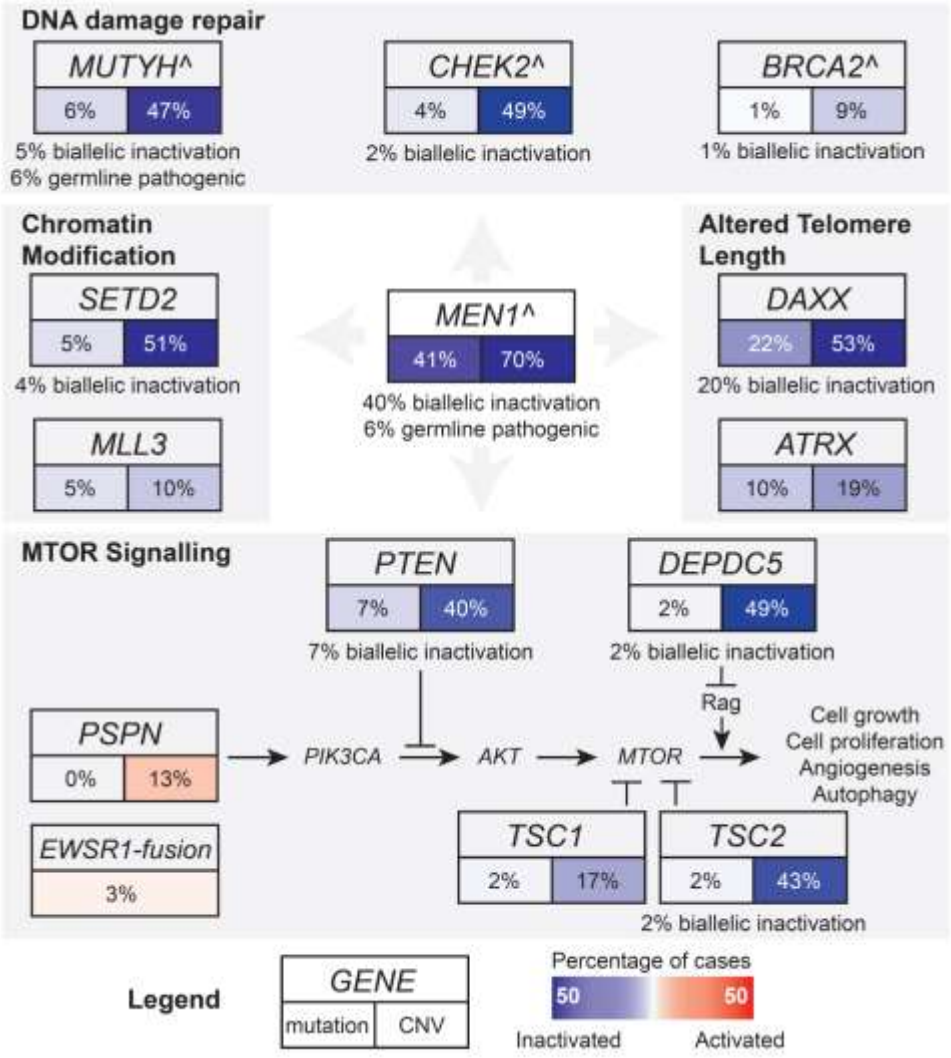

Fig. 10 | Core pathways in pancreatic neuroendocrine tumours. The frequency of somatic mutations and copy number change are shown in key genes of the mTOR signalling pathway, histone modification, altered telomere length and DNA damage repair pathways. *MEN1*, which is frequently mutated in pancreatic neuroendocrine tumours is involved in all these processes. Activating changes (red) include copy number change of 6 or more and inactivating changes (blue) include copy number 1 or copy number two with LOH. Genes that also contain germline variants predicted as pathogenic are shown (^). *ATRX* is located on chromosome X and showed point mutations in 6 males and 4 females, and in three of the females the inactivation was biallelic by LOH (*).

Table 1

Summary of clinicopathological variable and outcome analysis for 98 pancreatic neuroendocrine tumours patients.

	PanNET Whole Cohort					PanNET G2 Cohort				
Variables	**n = 98 No. (%)**	**Median DSS (mth)**	***P* value (Logrank)**	**Hazard Ratio (95% CI)**	***P* value**	**n = 57 No. (%)**	**Median DSS (mth)**	***P* value (Logrank)**	**Hazard Ratio (95% CI)**	***P* value**
Sex										
Female	35 (35.7)	----[a]		1		21 (36.8)	----		1	
Male	63 (64.3)	----	0,22	2.55 (0.54 – 12.0)	0,2368	36 (63.2)	----	0,2577		
Age (years)										
Mean	59					55,4				
Median	59					56				
Range	17.0–87.0					20.0–77.0				
Outcome										
Follow-up (months)	0.1–178					1.3–178				
Median follow-up	35,6					36,1				
Alive without Dx	47 (48.0)					25 (43.9)				
Alive with Dx	24 (24.5)					20 (35.1)				
Alive Dx Unknown	11 (11.2)					6 (10.5)				
Death PNET	10 (10.2)					5 (8.8)				
Death Other	4 (4.1)					1 (1.8)				
Death Unknown	1 (1.0)					0 (0)				
Lost to Follow-Up	1 (1.0)					0 (0)				
Stage										
IA	12 (12.2)					2 (3.5)				
IB	30 (30.6)	----				16 (28.1)	----			
IIA	10 (10.2)					8 (14.0)				
IIB	27 (27.6)	----				18 (31.6)	----			
III	1 (1.0)	----				1 (1.8)	----			
IV	18 (18.4)	72,5	XXXX			12 (21.1)	72,5	XXXX		
T Stage										
T1	13 (13.3)					3 (5.3)				
T2	48 (49.0)	----		1		30 (52.6)	----		1	
T3	34 (34.7)					22 (38.6)				
T4	3 (3.1)	----	0,0165	4.52 (1.17 – 17.5)	0,0288	2 (3.5)	----	0,0862	5.56 (0.62 – 50)	0,1268
N Stage										
N0	50 (52.1)	----		1		23 (41.8)	----			
N1	46 (47.9)	----	0,0661	3.89 (0.82 – 18.5)	0,0877	32 (58.2)	----	XXXX		XXXX
M Stage										
M0	80 (81.6)	----		1		45 (78.9)				
M1	18 (18.4)	72,5	<0.0001	35.7 (4.46 - 250)	0,0007	12 (21.1)	72,5	XXXX		XXXX
WHO Grade										
G1	36 (36.7)	----								
G2	57 (58.2)	----		1						
G3	5 (5.1)	9,4	<0.0001	24.4 (5.21 – 111)	0,0152					
Tumour size										
≤ 20mm	19 (19.4)					7 (12.3)				
20 – 40mm	35 (35.7)	----		1		21 (36.8)	----		1	
> 40mm	44 (44.9)	----	0.0273	4.85 (1.03 – 22.7)	0,046	29 (50.9)	----	0,2119	3.69 (0.41 – 33.3)	0,244
Extra-Panc Spread										
Absent	53 (54.1)	----		1		28 (49.1)	----			
Present	45 (45.9)	----	0.0036	11.36 (1.44 – 90.9)	0,0212	29 (50.9)	----	XXXX		XXXX
Margins										
Clear	84 (86.6)	----		1		49 (87.5)	----		1	
Involved	13 (13.4)	72,5	0.0019	6.25 (1.66 – 23.8)	0.0067	7 (12.5)	72,5	0,0347	6.41 (0.89 – 45.5)	0,0653
Perineural Invasion										
Negative	50 (58.1)	----				29 (59.2)	----			
Positive	36 (41.9)	----	XXXX		XXXX	20 (40.8)	----	XXXX		XXXX
Vascular Invasion										
Negative	37 (40.2)	----				16 (30.2)	----			
Positive	55 (59.8)	----	XXXX		XXXX	37 (69.8)	----	XXXX		XXXX

a ---- Median survival has not been reached.
XXXX = P value cannot be generated as the better prognosis arm did not have any events.

Table 1 (continues)

	PanNET Whole Cohort					PanNET G2 Cohort				
Variables	n = 98 No. (%)	Median DSS (mth)	*P* value (Logrank)	Hazard Ratio (95% CI)	*P* value	n = 57 No. (%)	Median DSS (mth)	*P* value (Logrank)	Hazard Ratio (95% CI)	*P* value
ALT (c-circle)										
Negative	54 (62.8)	----		1		23 (48.9)	----		1	
Positive	32 (37.2)	----	0.9989	1.0 (0.24 – 4.20)	0.9989	24 (51.1)	----	0.9921	1.01 (0.14 – 7.19)	0.9921
MEN1 (somatic)										
WT	63 (64.3)	----		1		36 (63.2)	----		1	
Mutant	35 (35.7)	----	0.879	0.90 (0.23 – 3.48)	0.8791	21 (36.8)	----	0.6568	1.50 (0.25 – 8.93)	0.6589
MEN1 (S or GL)										
WT	57 (58.2)	----		1		32 (56.1)	----		1	
Mutant	41 (41.8)	----	0.4623	0.60 (0.16 – 2.35)	0.4669	25 (43.9)	----	0.838	0.83 (0.14 – 5.03)	0.8382
DAXX (somatic)										
WT	76 (77.6)	----		1		39 (68.4)	----		1	
Mutant	22 (22.4)	----	0.4905	1.60 (0.41 – 6.21)	0.4944	18 (31.6)	----	0.6167	1.57 (0.26 – 9.43)	0.6196
ATRX (somatic)										
WT	87 (88.8)	----		1		49 (86.0)	----		1	
Mutant	11 (11.2)	72.5	0.0987	2.97 (0.77 – 11.5)	0.1157	8 (14.0)	51.6	0.001	11.2 (1.84 – 66.7)	0.0087
DAXX or ATRX										
WT	65 (66.3)	----		1		31 (54.4)	----			
Mutant	33 (33.7)	----	0.0792	2.95 (0.83 – 10.4)	0.0943	26 (45.6)	----	XXXX		XXXX
MEN1/DAXX/ATRX										
WT	43 (43.9)	----		1		20 (35.1)	----			
Mutant	55 (56.1)	----	0.8992	1.09 (0.31 – 3.86)	0.8993	37 (64.9)	----	XXXX		XXXX
mTOR Pwy (mTOR, TSC1, TSC2, DEPDC5, PTEN)										
WT	83 (84.7)	----		1		45 (78.9)	----		1	
Mutant	15 (15.3)	----	0.304	2.00 (0.52 – 7.75)	0.3136	12 (21.1)	----	0.0395	5.41 (0.89 – 32.3)	0.066
mTOR Pway (excl. mTOR)										
WT	86 (87.8)	----		1		47 (82.5)	----		1	
Mutant	12 (12.2)	----	0.1596	2.55 (0.66 – 9.90)	0.1749	10 (17.5)	----	0.0148	6.85 (1.14 – 41.7)	0.0353

a ---- Median survival has not been reached.
XXXX = P value cannot be generated as the better prognosis arm did not have any events.

Table 2

Summary of DAXX/ATRX mutational status correlation to clinico-pathological variables.

DAXX/ATRX Correlation	PNET Whole Cohort (N = 98)		PNET G2 Cohort (N = 57)	
Variables	*P* value (Chi-Square)	KM Significant	*P* value (Chi-Square)	KM Significant
T3/4	0,0146	Y	0,5707	N
N1	0,0039	N	0,4246	XXXX
M1	0,0064	Y	0,0214	XXXX
Size > 40mm	0,0004	Y	0,0111	N
Extra-Panc spread	0,0033	Y	0,3459	XXXX
Margin Involvement	0,0186	Y	0,0194	N
Perineural Invasion	0,0246	XXXX	0,0188	XXXX
Vascular Invasion	0,0088	XXXX	0,3537	XXXX
WHO Grade 2/3	0,0231	Y	NA	NA
ALT (c-circle) Positive	< 0.0001	N	< 0.0001	N
mTOR Pway Mutants (mTOR, TSC1, TSC2, DEPDC5, PTEN)	0,0004	N	0,0214	N
mTOR Pway Mutants (excl. mTOR)	0,0012	N	0,0162	Y

Y = P ≤ 0.05

N = P > 0.05

XXXX = P value cannot be generated as the better prognosis arm did not have any events.

5. Methods

5.1 *Human research ethical approval*

ARC-Net, University of Verona: approval number 1885 from the Integrated University Hospital Trust (AOUI) Ethics Committee (Comitato Etico Azienda Ospedaliera Universitaria Integrata) approved in their meeting of 17 November 2010 and documented by the ethics committee 52070/CE on 22 November 2010 and formalized by the Health Director of the AOUI on the order of the General Manager with protocol 52438 on 23 November 2010. *APGI*: Sydney South West Area Health Service Human Research Ethics Committee, western zone (protocol number 2006/54); Sydney Local Health District Human Research Ethics Committee (X11-0220); Northern Sydney Central Coast Health Harbour Human Research Ethics Committee (0612-251M); Royal Adelaide Hospital Human Research Ethics Committee (091107a); Metro South Human Research Ethics Committee (09/QPAH/220); South Metropolitan Area Health Service Human Research Ethics Committee (09/324); Southern Adelaide Health Service/Flinders University Human Research Ethics Committee (167/10); Sydney West Area Health Service Human Research Ethics Committee (Westmead campus) (HREC2002/3/4.19); The University of Queensland Medical Research Ethics Committee (2009000745); Greenslopes Private Hospital Ethics Committee (09/34); North Shore Private Hospital Ethics Committee. *Baylor College of Medicine*: Institutional Review Board protocol numbers H-29198 (Baylor College of Medicine tissue resource), H-21332 (Genomes and Genetics at the BCM-HGSC), and H-32711(Cancer Specimen Biobanking and Genomics).

5.2 *PanNET Patient and Tissue Cohort*

Patients were recruited and consent obtained for genomic sequencing through the ARC-Net Research Centre at Verona University, Australian Pancreatic Cancer Genome Initiative (APGI), and Baylor College of Medicine as part of the ICGC (www.icgc.org). A patient criterion for admission to the study was that they were clinically sporadic. This information was acquired through direct interviews with participants and a questionnaire regarding their

personal history and that of relatives with regard to pancreas cancers and any other cancers during anamnesis. Investigations were also done on clinical records to clarify familial history based on the patient indication.

Samples were prospectively and consecutively acquired through institutions affiliated with the Australian Pancreatic Cancer Genome Initiative. Samples from the ARC-Net biobank are the result of a consecutive collection from a single centre.

All tissue samples were processed as previously described(66). Representative sections were reviewed independently by at least one additional pathologist with specific expertise in pancreatic diseases. Samples either had full face frozen sectioning performed in optimal cutting temperature (OCT) medium, or the ends excised and processed in formalin to verify the presence of tumour in the sample to be sequenced and to estimate the percentage of neoplastic cells in the sample relative to stromal cells. Macrodissection was performed if required to excise areas that did not contain neoplastic epithelium. Tumour cellularity was determined using SNP arrays (Illumina, San Diego) and the qpure tool(25).

5.3 *Sample size*

PanNET is rare tumour type and the samples have been collected via an International Network. We estimate that with 98 unique patients in the discovery cohort, we will achieve 90% power for 90% of genes to detect mutations that occur at a frequency of ~10% above the background rate for PanNET (assuming a somatic mutation frequency of < 2 per Mb)(67).

5.4 *Colon sample acquisition*

Cancer and matched normal colonic mucosa were collected at the time of surgical resection from the Royal Brisbane and Women's Hospital and snap frozen in liquid nitrogen. A biallelic germline mutation in the *MUTYH* gene was detected by restriction fragment length polymorphism analysis and confirmed by automated sequencing to be the G382D mutation (or ENST00000372098 G393D) in both alleles(68).

5.5 *Immunohistochemistry*

The primary antibodies used for immunohistochemical staining were: Cytokeratin 8/18 (5D3, Novocastra), Chromogranin A (DAK-A3, Dako), and CD99 (O13, Biolegend). Antibodies and staining conditions have been described elsewhere(53).

5.6 *Sequencing and mutation analysis*

Matched tumour/normal DNAs underwent whole genome sequencing (WGS) (average 38x normal/61x tumour) and high-density SNP arrays (data not shown), and orthogonal testing estimated the accuracy of somatic calls to exceed 99%. Whole genome sequencing with 100bp paired reads was performed with a HiSEQ2000 (Illumina, San Diego). Sequence data was mapped to a GRCh37 using BWA and BAM files are available in the EGA (Accession number: EGAS00001001732). Somatic mutations and germline variants were detected using a previously described consensus mutation calling strategy(30). Mutations were annotated with gene consequence using SNPeff. The pathogenicity of germline variants was predicted using cancer-specific and locus-specific genetic databases, medical literature, computational predictions with ENSEMBL Variant Effect Predictor (VEP) annotation, and second hits identified in the tumour genome. Intogen(41) was used to find somatic genes which were significantly mutated. Structural rearrangements were detected by integrating discordant read pairs, soft-clipping, split read & de novo assembly of non-mapping reads using the qSV tool as previously described(30, 31). Coding mutations are included in supplementary tables (data not shown) and all mutations have been uploaded to the ICGC DCC.

5.7 *Mutational signature*

Mutational signatures were predicted using a published framework(27). Essentially the 96 substitution classification was determined for each sample.

The signatures were compared to other validated signatures and the prevalence of each signature per Mb was determined.

5.8 *Copy number analysis*

Somatic copy number was estimated using high density SNP arrays and the GAP tool(69). Arm level copy number data was clustered using Ward's method, Euclidian distance. GISTIC(70) was used to identify recurrent regions of copy number change.

5.9 *Telomere length*

The whole genome sequence data was used to determine the length of the telomeres in each sample using the qMotif tool. Essentially, qMotif determines telomeric DNA content by calculating the number of reads which harbour the telomere motif (TTAGG), and then estimates the relative length of telomeres in the tumour compared to the normal. qMotif is available online (http://sourceforge.net/projects/adamajava). Telomere length was validated by qPCR as previously described(71).

5.10 *Validation of fusion transcripts*

Two different strategies were used to verify fusion transcripts. For verification of *EWSR1-BEND2* fusions, cDNAs were synthesized by using the SuperScript VILO cDNA synthesis kit (Thermofisher) with 1µg of purified total RNA. For each fusion sequence three samples were used: the PanNET sample containing the fusion, the PanNET sample without that fusion, and a non-neoplastic pancreatic sample. The RT-PCR product were evaluated on the Agilent 2100 Bioanalyzer (Agilent Technologies) and verified by sequencing using the 3130XL Genetic Analyzer (Life Technologies). Primers specific for *EWSR1-BEND2* fusion genes are available upon request. To identify the *EWSR1* fusion partner in the case ITNET_2045, a real-time RT-PCR translocation panel for detecting specific Ewing sarcomas fusion transcripts was applied as described(72). Following identification of the

fusion partner, PCR amplicons were subjected to sequencing using the 3130XL Genetic Analyzer.

5.11 *Fluorescent in situ hybridization (FISH) analysis*

EWSR1 rearrangements were assayed on paraffin-embedded tissue sections using a commercial split-signal probe (Vysis LSI EWSR1 (22q12) Dual Color, Break Apart Rearrangement FISH Probe Kit) that consists of a mixture of two FISH DNA probes. One probe (~500 kb) is labelled in SpectrumOrange and flanks the 5' side of the *EWSR1* gene, extending through intron 4, and the second probe (~1100 kb) is labelled in SpectrumGreen and flanks the 3' side of the *EWSR1* gene, with a 7 kb gap between the two probes. With this setting, the assay enables the detection of rearrangements with breakpoints spanning introns 7 to 10 of the *EWSR1* gene. Hybridization was performed according to the manufacturer's instructions and scoring of tissue sections was assessed as described elsewhere(73), counting at least 100 nuclei per slide.

5.12 *Targeted sequencing*

Recurrently mutated genes identified by whole genome sequencing were independently evaluated in a series of 62 PaNETs from the ARC-Net Research Centre, University of Verona. Four Ion Ampliseq Custom panel (Thermofisher) were designed to target the entire coding regions and flanking intron-exon junctions of the following genes: *MEN1, DAXX, ATRX, PTEN*, and *TSC2* (panel 1); *DEPDC5*, *TSC1*, and *SETD2* (panel 2); *ARID1A* and *MTOR* (panel 3); *CHEK2* and *MUTYH* (panel 4). Twenty nanograms of DNA were used per multiplex PCR amplification. The quality of the obtained libraries was evaluated by the Agilent 2100 Bioanalyzer on chip electrophoresis. Emulsion PCR was performed with the OneTouch system (Thermofisher). Sequencing was run on the Ion Torrent Personal Genome Machine (PGM, Thermofisher) loaded with 316 or 318 chips. Data analysis, including alignment to the hg19 human reference genome and variant calling, was done using Torrent Suite Software v4.0 (Thermofisher). Filtered variants

were annotated using a custom pipeline based on the Variant Effector Predictor (VEP) software. Alignments were visually verified with the Integrative Genomics Viewer: IGV v2.3 (Broad Institute).

5.13 *Clinical correlations*

The date of diagnosis and the date and cause of death were obtained from the Central Cancer Registry and treating clinicians. Median survival was estimated using the Kaplan-Meier method and the difference was tested using the log-rank Test. *P* values of less than 0.05 were considered statistically significant. Hazard ratio and its 95% confidence interval was estimated using Cox proportional hazard regression modelling. The correlation between *DAXX/ATRX* mutational status with other clinico-pathological variables was performed using Chi-squared test. Statistical analysis was performed using StatView 5.0 Software (Abacus Systems, Berkeley, CA, USA). Disease-specific survival was used as the primary endpoint.

6. Aknowledgments

Volevo ringraziare il Prof. A. Scarpa, perché è stato per me mentore e maestro, trasmettendomi la passione per la ricerca e la gioia di chi svolge il proprio "mestiere" con passione e perché no, un pizzico di follia, insegnandomi la tenacia nel perseguire gli obiettivi e la forza di sostenere le proprie idee, a dispetto di quanti ti possano remare contro. Perché ha sempre creduto in me e mi ha permesso di crescere professionalmente e umanamente: grazie prof!

Grazie anche a Vincenzo Corbo, perchè mi è stato vicino nel mio percorso di formazione, aiutandomi a superare i limiti e ad affrontare le difficoltà con un sorriso. Discutere di scienza con te è sempre stato costruttivo e stimolante e per me è davvero motivo di orgoglio l'aver avuto la possibilità di lavorare con te..

Un ringraziamento va anche ad Andrea Mafficini, per cui nutro una immensa stima professionale, che non solo è un eccellente professionista, un ottimo insegnante e un paziente consigliere, ma prima di tutto è davvero una persona meravigliosa.

Volevo ringraziare anche Borislav Rusev, uomo saggio e patologo dalle eccellenti qualità, mi ha guidato nelle insidie di questo mestiere e mi ha sempre dato buoni consigli.

Grazie anche a Rita Lawlor, che con la sua straordinaria capacità manageriale si è sempre prodigata per far si che ARC-NET diventasse il fiore all'occhiello della ricerca italiana. Con lei volevo ringraziare anche tutta la squadra di ARC-NET (Cinzia, Giada, Sonia, Paola, Francesca, Nicola) per l'eccellente lavoro che svolgono ogni giorno e perché sono stati amici, oltre che collaboratori.

Un ringraziamento a tutti i ragazzi del lab., Eliana, Samantha, Maria, Marina, Giona, Dea, Reka, Michele, Davide, Liliana, Manuele, Carla, Caterina, Claudia e Stefano e perché abbiamo condiviso tanti momenti belli e mi hanno aiutato a vivere con leggerezza quelli meno piacevoli.

Un grazie va a Paolo Dei Tos, per la fiducia che ha riposto in me.

Dulcis in fundo, un ringraziamento particolare va alla mia famiglia, primi tra tutti mio marito Filippo e mio figlio Vincenzo perché con voi "io ho tutto quello che mi serve per essere felice".

7. References

1. Modlin IM SM, Kidd M Siegfried Oberndorfer: origins and perspectives of carcinoid tumors. . Hum Pathology 2004;35(12):1440–51.
2. Taal BG VO. Epidemiology of neuroendocrine tumours. . Neuroendocrinology 2004;80 (Suppl 1):3–7.
3. SEER Survival Monograph: Cancer Survival Among Adults: U.S. SEER Program, 1988-2001, Patient and Tumor Characteristics. National Cancer Institute, SEER Program, . Ries LAG YJ, Keel GE, Eisner MP, Lin YD, Horner M-J editor. Bethesda, MD: NIH Pub. No. 07-6215,; 2007.
4. Kilickap S, Hayran KM. Epidemiology of Neuroendocrine Tumours. In: Yalcin S, Öberg K, editors. Neuroendocrine Tumours: Diagnosis and Management. Berlin, Heidelberg: Springer Berlin Heidelberg; 2015. p. 513-22.
5. Bosman FT, Carneiro F, Hruban RH, Theise ND. WHO Classification of Tumours of the Digestive System. 4th ed. Lyon: International Agency for Research on Cancer (IARC); 2010.
6. Yachida S VE, White CM, Zhong Y, Saunders T, Morgan R, de Wilde RF, Maitra A, Hicks J, Demarzo AM, Shi C, Sharma R, Laheru D, Edil BH, Wolfgang CL, Schulick RD, Hruban RH, Tang LH, Klimstra DS, Iacobuzio-Donahue CA. Small cell and large cell neuroendocrine carcinomas of the pancreas are genetically similar and distinct from well-differentiated pancreatic neuroendocrine tumors. The American journal of surgical pathology. 2012;36(2):173-84.
7. TNM classification of malignant tumours 7th ed. Sobin LHG, M K (Mary K); Wittekind, Ch (Christian); International Union against Cancer., editor. Chichester, West Sussex, UK ; Hoboken, NJ : : Wiley-Blackwell; 2010.
8. Klöppel G RG, Perren A, Komminoth P, Klimstra DS. The ENETS and AJCC/UICC TNM classifications of the neuroendocrine tumors of the gastrointestinal tract and the pancreas: a statement. Virchows Arch 2010;Jun;456(6):595-7.
9. Scarpa A, Corbo Vincenzo, Barbi Stefano, Cataldo Ivana, Fassan Matteo Molecular Biology of Neuroendocrine Tumours. In: Yalcin S, Öberg K, editors. Neuroendocrine Tumours: Diagnosis and Management. Berlin, Heidelberg: Springer Berlin Heidelberg; 2015. p. 35-49.
10. Neuroendocrine Tumors: A Multidisciplinary Approach. . Papotti M. dHW, editor: Front Horm Res. Basel, Karger, 2015, .
11. Chandrasekharappa SC GS, Manickam P, Olufemi SE, Collins FS, Emmert-Buck MR, Debelenko LV, Zhuang Z, Lubensky IA, Liotta LA, Crabtree JS, Wang Y, Roe BA,

Weisemann J, Boguski MS, Agarwal SK, Kester MB, Kim YS, Heppner C, Dong Q, Spiegel AM, Burns AL, Marx SJ. Positional cloning of the gene for multiple endocrine neoplasia-type 1. Science. 1997 Apr 18;276(5311):404-7.

12. Jiao Y, Shi C, Edil BH, de Wilde RF, Klimstra DS, Maitra A, et al. DAXX/ATRX, MEN1, and mTOR pathway genes are frequently altered in pancreatic neuroendocrine tumors. Science. 2011;331(6021):1199-203.

13. Corbo V DI, Scardoni M, Barbi S, Beghelli S, Bersani S, Albarello L, Doglioni C, Schott C, Capelli P, Chilosi M, Boninsegna L, Becker KF, Falconi M, Scarpa A. MEN1 in pancreatic endocrine tumors: analysis of gene and protein status in 169 sporadic neoplasms reveals alterations in the vast majority of cases. Endocr Relat Cancer. 2010;Aug 16;17(3):771-8.

14. Corbo V BS, Bersani S, Antonello D, Talamini G, Brunelli M, Capelli P, Falconi M, Scarpa A. Pancreatic endocrine tumours: mutational and immunohistochemical survey of protein kinases reveals alterations in targetable kinases in cancer cell lines and rare primaries. Ann Oncol. 2012;Jan 23(1):127-34.

15. Schmitt AM SS, Rudolph T, Anlauf M, Prinz C, Klöppel G, Moch H, Heitz PU, Komminoth P, Perren A. VHL inactivation is an important pathway for the development of malignant sporadic pancreatic endocrine tumors. Endocr Relat Cancer. 2009;Dec 16(4):1219-27.

16. Jonkers YM RF, Speel EJ. Molecular alterations during insulinoma tumorigenesis. Biochim Biophys Acta. 2007;Jun;1775((2)):313-32.

17. Elsässer SJ AC, Lewis PW. Cancer. New epigenetic drivers of cancers. Science. 2011;Mar 4;331(6021):1145-6.

18. Heaphy CM dWR, Jiao Y, Klein AP, Edil BH, Shi C, Bettegowda C, Rodriguez FJ, Eberhart CG, Hebbar S, Offerhaus GJ, McLendon R, Rasheed BA, He Y, Yan H, Bigner DD, Oba-Shinjo SM, Marie SK, Riggins GJ, Kinzler KW, Vogelstein B, Hruban RH, Maitra A, Papadopoulos N, Meeker AK. Altered telomeres in tumors with ATRX and DAXX mutations. Science. 2011;Jul 22;333(6041):425.

19. de Wilde RF HC, Maitra A, Meeker AK, Edil BH, Wolfgang CL, Ellison TA, Schulick RD, Molenaar IQ, Valk GD, Vriens MR, Borel Rinkes IH, Offerhaus GJ, Hruban RH, Matsukuma KE. Loss of ATRX or DAXX expression and concomitant acquisition of the alternative lengthening of telomeres phenotype are late events in a small subset of MEN-1 syndrome pancreatic neuroendocrine tumors. Mod Pathol. 2012; 2012 Jul;25(7):1033-9.

20. Marinoni I KA, Vassella E, Dettmer M, Rudolph T, Banz V, Hunger F, Pasquinelli S, Speel EJ, Perren A. Loss of DAXX and ATRX are associated with chromosome instability and reduced survival of patients with pancreatic neuroendocrine tumors. Gastroenterology. 2014;Feb;146(2):453-60.e5.

21. Fernandes I PT, Costa A, Santos AC, Fernandes AR, Santos M, Oliveira AG, Casimiro S, Quintela A, Fernandes A, Ramos M, Costa L. Prognostic significance of AKT/mTOR signaling in advanced neuroendocrine tumors treated with somatostatin analogs. Onco Targets Ther. 2012;5:409-16.

22. Komori Y YK, Ohta M, Uchida H, Iwashita Y, Fukuzawa K, Kashima K, Yokoyama S, Inomata M, Kitano S. Mammalian target of rapamycin signaling activation patterns in pancreatic neuroendocrine tumors. J Hepatobiliary Pancreat Sci 2014;Apr;21(4):288-95.

23. Missiaglia E, Dalai I, Barbi S, Beghelli S, Falconi M, della Peruta M, et al. Pancreatic endocrine tumors: expression profiling evidences a role for AKT-mTOR pathway. J Clin Oncol. 2010;28(2):245-55.

24. Neychev V, Steinberg SM, Cottle-Delisle C, Merkel R, Nilubol N, Yao J, et al. Mutation-targeted therapy with sunitinib or everolimus in patients with advanced low-grade or intermediate-grade neuroendocrine tumours of the gastrointestinal tract and pancreas with or without cytoreductive surgery: protocol for a phase II clinical trial. BMJ Open. 2015;5(5):e008248.

25. Song S, Nones K, Miller D, Harliwong I, Kassahn KS, Pinese M, et al. qpure: A Tool to Estimate Tumor Cellularity from Genome-Wide Single-Nucleotide Polymorphism Profiles. PLoS One. 2012;7(9):e45835.

26. Waddell N, Pajic M, Patch AM, Chang DK, Kassahn KS, Bailey P, et al. Whole genomes redefine the mutational landscape of pancreatic cancer. Nature. 2015;518(7540):495-501.

27. Alexandrov LB, Nik-Zainal S, Wedge DC, Aparicio SA, Behjati S, Biankin AV, et al. Signatures of mutational processes in human cancer. Nature. 2013;500(7463):415-21.

28. Nik-Zainal S, Alexandrov LB, Wedge DC, Van Loo P, Greenman CD, Raine K, et al. Mutational processes molding the genomes of 21 breast cancers. Cell. 2012;149(5):979-93.

29. Nik-Zainal S, Davies H, Staaf J, Ramakrishna M, Glodzik D, Zou X, et al. Landscape of somatic mutations in 560 breast cancer whole-genome sequences. Nature. 2016;534(7605):47-54.

30. Patch AM, Christie EL, Etemadmoghadam D, Garsed DW, George J, Fereday S, et al. Whole-genome characterization of chemoresistant ovarian cancer. Nature. 2015;521(7553):489-94.

31. Nones K, Waddell N, Wayte N, Patch AM, Bailey P, Newell F, et al. Genomic catastrophes frequently arise in esophageal adenocarcinoma and drive tumorigenesis. Nature communications. 2014;5:5224.

32. Al-Tassan N, Chmiel NH, Maynard J, Fleming N, Livingston AL, Williams GT, et al. Inherited variants of MYH associated with somatic G:C-->T:A mutations in colorectal tumors. Nat Genet. 2002;30(2):227-32.

33. Aretz S, Tricarico R, Papi L, Spier I, Pin E, Horpaopan S, et al. MUTYH-associated polyposis (MAP): evidence for the origin of the common European mutations p.Tyr179Cys and p.Gly396Asp by founder events. Eur J Hum Genet. 2014;22(7):923-9.

34. Vogt S, Jones N, Christian D, Engel C, Nielsen M, Kaufmann A, et al. Expanded extracolonic tumor spectrum in MUTYH-associated polyposis. Gastroenterology. 2009;137(6):1976-85 e1-10.

35. Stephens PJ, Greenman CD, Fu B, Yang F, Bignell GR, Mudie LJ, et al. Massive genomic rearrangement acquired in a single catastrophic event during cancer development. Cell. 2011;144(1):27-40.

36. Rausch T, Jones DT, Zapatka M, Stutz AM, Zichner T, Weischenfeldt J, et al. Genome sequencing of pediatric medulloblastoma links catastrophic DNA rearrangements with TP53 mutations. Cell. 2012;148(1-2):59-71.

37. Georgitsi M, Raitila A, Karhu A, van der Luijt RB, Aalfs CM, Sane T, et al. Germline CDKN1B/p27Kip1 mutation in multiple endocrine neoplasia. J Clin Endocrinol Metab. 2007;92(8):3321-5.

38. Francis JM, Kiezun A, Ramos AH, Serra S, Pedamallu CS, Qian ZR, et al. Somatic mutation of CDKN1B in small intestine neuroendocrine tumors. Nat Genet. 2013;45(12):1483-6.

39. Lubensky IA, Pack S, Ault D, Vortmeyer AO, Libutti SK, Choyke PL, et al. Multiple neuroendocrine tumors of the pancreas in von Hippel-Lindau disease patients: histopathological and molecular genetic analysis. Am J Pathol. 1998;153(1):223-31.

40. Dong X, Wang L, Taniguchi K, Wang X, Cunningham JM, McDonnell SK, et al. Mutations in CHEK2 associated with prostate cancer risk. American journal of human genetics. 2003;72(2):270-80.

41. Gonzalez-Perez A, Perez-Llamas C, Deu-Pons J, Tamborero D, Schroeder MP, Jene-Sanz A, et al. IntOGen-mutations identifies cancer drivers across tumor types. Nature methods. 2013;10(11):1081-2.

42. Gerlinger M, Rowan AJ, Horswell S, Larkin J, Endesfelder D, Gronroos E, et al. Intratumor heterogeneity and branched evolution revealed by multiregion sequencing. N Engl J Med. 2012;366(10):883-92.

43. Win AK, Lindor NM, Winship I, Tucker KM, Buchanan DD, Young JP, et al. Risks of Colorectal and Other Cancers After Endometrial Cancer for Women With Lynch Syndrome. Journal of the National Cancer Institute. 2013;105(4):274-9.

44. Tang M, Shen H, Jin Y, Lin T, Cai Q, Pinard MA, et al. The malignant brain tumor (MBT) domain protein SFMBT1 is an integral histone reader subunit of the LSD1 demethylase complex for chromatin association and epithelial-to-mesenchymal transition. J Biol Chem. 2013;288(38):27680-91.

45. Asai A, Karnan S, Ota A, Takahashi M, Damdindorj L, Konishi Y, et al. High-resolution 400K oligonucleotide array comparative genomic hybridization analysis of neurofibromatosis type 1-associated cutaneous neurofibromas. Gene. 2015;558(2):220-6.

46. Baba T, Sakamoto Y, Kasamatsu A, Minakawa Y, Yokota S, Higo M, et al. Persephin: A potential key component in human oral cancer progression through the RET receptor tyrosine kinase-mitogen-activated protein kinase signaling pathway. Mol Carcinog. 2015;54(8):608-17.

47. Lindahl M, Poteryaev D, Yu L, Arumae U, Timmusk T, Bongarzone I, et al. Human glial cell line-derived neurotrophic factor receptor alpha 4 is the receptor for persephin and is predominantly expressed in normal and malignant thyroid medullary cells. J Biol Chem. 2001;276(12):9344-51.

48. Alers S, Loffler AS, Wesselborg S, Stork B. Role of AMPK-mTOR-Ulk1/2 in the regulation of autophagy: cross talk, shortcuts, and feedbacks. Mol Cell Biol. 2012;32(1):2-11.

49. Sturm D, Orr BA, Toprak UH, Hovestadt V, Jones DT, Capper D, et al. New Brain Tumor Entities Emerge from Molecular Classification of CNS-PNETs. Cell. 2016;164(5):1060-72.

50. May WA, Gishizky ML, Lessnick SL, Lunsford LB, Lewis BC, Delattre O, et al. Ewing sarcoma 11;22 translocation produces a chimeric transcription factor that requires the DNA-binding domain encoded by FLI1 for transformation. Proceedings of the National Academy of Sciences of the United States of America. 1993;90(12):5752-6.

51. Sankar S LS. Promiscuous partnerships in Ewing's sarcoma. Cancer Genet. 2011; Jul;204(7):351-65.

52. Delattre O, Zucman J, Plougastel B, Desmaze C, Melot T, Peter M, et al. Gene fusion with an ETS DNA-binding domain caused by chromosome translocation in human tumours. Nature. 1992;359(6391):162-5.

53. Stockman DL, Miettinen M, Suster S, Spagnolo D, Dominguez-Malagon H, Hornick JL, et al. Malignant gastrointestinal neuroectodermal tumor: clinicopathologic, immunohistochemical, ultrastructural, and molecular analysis of 16 cases with a reappraisal of clear cell sarcoma-like tumors of the gastrointestinal tract. The American journal of surgical pathology. 2012;36(6):857-68.

54. WHO Classification of Tumours of Soft Tissue and Bone. Fourth Edition. Lyon: IARC; 2013.

55. Brohl AS SD, Chang W, Wang J, Song Y, Sindiri S, Patidar R, Hurd L, Chen L, Shern JF, Liao H, Wen X, Gerard J, Kim JS, Lopez Guerrero JA, Machado I, Wai DH, Picci P, Triche T, Horvai AE, Miettinen M, Wei JS, Catchpool D, Llombart-Bosch A, Waldman T, Khan J. The genomic landscape of the Ewing Sarcoma family of tumors reveals recurrent STAG2 mutation. PLoS Genet. 2014; Jul 10;10(7):e1004475.

56. Crompton BD SC, Taylor-Weiner A, Alexe G, Kurek KC, Calicchio ML, Kiezun A, Carter SL, Shukla SA, Mehta SS, Thorner AR, de Torres C, Lavarino C, Suñol M, McKenna A, Sivachenko A, Cibulskis K, Lawrence MS, Stojanov P, Rosenberg M, Ambrogio L, Auclair D, Seepo S, Blumenstiel B, DeFelice M, Imaz-Rosshandler I, Schwarz-Cruz Y Celis A, Rivera MN, Rodriguez-Galindo C, Fleming MD, Golub TR, Getz G, Mora J, Stegmaier K. The genomic landscape of pediatric Ewing sarcoma. Cancer Discov. 2014;Nov;4(11):1326-41.

57. Tirode F SD, Ma X, Parker M, Le Deley MC, Bahrami A, Zhang Z, Lapouble E, Grossetête-Lalami S, Rusch M, Reynaud S, Rio-Frio T6, Hedlund E, Wu G, Chen X, Pierron G, Oberlin O, Zaidi S, Lemmon G, Gupta P, Vadodaria B, Easton J, Gut M, Ding L, Mardis ER, Wilson RK, Shurtleff S, Laurence V, Michon J, Marec-Bérard P, Gut I9, Downing J Dyer M, Zhang J, Delattre O; St. Jude Children's Research Hospital-Washington University Pediatric Cancer Genome Project and the International Cancer Genome Consortium. Genomic landscape of Ewing sarcoma defines an aggressive subtype with co-association of STAG2 and TP53 mutations. Cancer Discov 2014;Nov;4(11):1342-53.

58. Goto A NT, Terado Y, Fukushima J, Fukayama M. Prevalence of CD99 protein expression in pancreatic endocrine tumours (PETs). Histopathology. 2004;Oct;45(4):384-92.

59. Pelosi G1 FF, Sonzogni A, Fazio N, Cavallon A, Viale G. CD99 immunoreactivity in gastrointestinal and pulmonary neuroendocrine tumours. Virchows Arch 2000;Sep;437(3):270-4.

60. Lovejoy CA, Li W, Reisenweber S, Thongthip S, Bruno J, de Lange T, et al. Loss of ATRX, genome instability, and an altered DNA damage response are hallmarks of the alternative lengthening of telomeres pathway. PLoS Genet. 2012;8(7):e1002772.

61. Lin SY, Elledge SJ. Multiple tumor suppressor pathways negatively regulate telomerase. Cell. 2003;113(7):881-9.

62. Bar-Peled L, Chantranupong L, Cherniack AD, Chen WW, Ottina KA, Grabiner BC, et al. A Tumor suppressor complex with GAP activity for the Rag GTPases that signal amino acid sufficiency to mTORC1. Science. 2013;340(6136):1100-6.

63. Fang M, Xia F, Mahalingam M, Virbasius CM, Wajapeyee N, Green MR. MEN1 is a melanoma tumor suppressor that preserves genomic integrity by stimulating transcription of genes that promote homologous recombination-directed DNA repair. Mol Cell Biol. 2013;33(13):2635-47.

64. Wang Y, Ozawa A, Zaman S, Prasad NB, Chandrasekharappa SC, Agarwal SK, et al. The tumor suppressor protein menin inhibits AKT activation by regulating its cellular localization. Cancer Res. 2011;71(2):371-82.

65. Matkar S, Thiel A, Hua X. Menin: a scaffold protein that controls gene expression and cell signaling. Trends in biochemical sciences. 2013;38(8):394-402.

66. Biankin AV, Waddell N, Kassahn KS, Gingras MC, Muthuswamy LB, Johns AL, et al. Pancreatic cancer genomes reveal aberrations in axon guidance pathway genes. Nature. 2012;491(7424):399-405.

67. Lawrence MS, Stojanov P, Mermel CH, Robinson JT, Garraway LA, Golub TR, et al. Discovery and saturation analysis of cancer genes across 21 tumour types. Nature. 2014;505(7484):495-501.

68. Kambara T, Whitehall VL, Spring KJ, Barker MA, Arnold S, Wynter CV, et al. Role of inherited defects of MYH in the development of sporadic colorectal cancer. Genes Chromosomes Cancer. 2004;40(1):1-9.

69. Popova T, Manie E, Stoppa-Lyonnet D, Rigaill G, Barillot E, Stern MH. Genome Alteration Print (GAP): a tool to visualize and mine complex cancer genomic profiles obtained by SNP arrays. Genome Biol. 2009;10(11):R128.

70. Mermel CH, Schumacher SE, Hill B, Meyerson ML, Beroukhim R, Getz G. GISTIC2.0 facilitates sensitive and confident localization of the targets of focal somatic copy-number alteration in human cancers. Genome Biol. 2011;12(4):R41.

71. O'Callaghan NJ, Fenech M. A quantitative PCR method for measuring absolute telomere length. Biological procedures online. 2011;13:3.

72. Lewis TB, Coffin CM, Bernard PS. Differentiating Ewing's sarcoma from other round blue cell tumors using a RT-PCR translocation panel on formalin-fixed paraffin-embedded tissues. Modern pathology : an official journal of the United States and Canadian Academy of Pathology, Inc. 2007;20(3):397-404.

73. Rossi S, Szuhai K, Ijszenga M, Tanke HJ, Zanatta L, Sciot R, et al. EWSR1-CREB1 and EWSR1-ATF1 fusion genes in angiomatoid fibrous histiocytoma. Clinical cancer research : an official journal of the American Association for Cancer Research. 2007;13(24):7322-8.